Simulating Quantum Light-Matter Interaction for Complex Systems in Optical Cavities

by
Nosheen Younas

A thesis submitted to the Department of Chemistry,
Collage of Natural Sciences and Mathematics
in partial fulfillment of the requirements for the degree of

Masters

in Chemistry

Chair of Committee: Dr. Eric R. Bittner

Committee Member: Dr. Vassiliy Lubchenko

Committee Member: Dr. Jakoah Brgoch

Committee Member: Dr. Judy I-Chia Wu

Committee Member: Dr. Carlos Silva

University of Houston
December 2020

DEDICATION/EPIGRAPH

TO MY HUSBAND, FOR HIS SUPPORT AND ENCOURAGEMENT.

ACKNOWLEDGMENTS

I am thankful to my mentor, Prof. Eric R. Bittner, for his immense support, guidance and patience. I am also grateful to Dr. Hao Li for his insightful inputs. This work could not have been possible without the generous financial support of the Welch Foundation.

ABSTRACT

Light-matter interaction is typically modeled in a semi-classical fashion where a classical electromagnetic field interacts with quantized matter. Although it is a powerful approach, it overlooks quantum mechanical features of light. A fully quantum mechanical treatment can be useful for probing the complex interactions within the matter. This project aims at modeling a fully quantum light-matter interaction in an open quantum system approach. The studied systems consist of material samples placed inside optical cavities that help enhance light-matter interaction as well as control the properties of light. The results reveal signatures of different intra-material interactions on the light emitted from the cavity. Particularly, the investigations focus on the effect of these interaction on spectral properties and statistical correlations of the emitted photons. Finally, a sample of much experimental and theoretical interest, the Light Harvesting Complex II, is studied with this approach. Ultimately, the relationships between observable properties of emitted light and intra-material interactions developed in these investigations can open new pathways for spectroscopy.

TABLE OF CONTENTS

DEDICATION/EPIGRAPH III
ACKNOWLEDGMENTS IV
TABLE OF CONTENTS VI
LIST OF TABLES VII
LIST OF FIGURES VIII
CHAPTER 1: INTRODUCTION 1
CHAPTER 2: QUANTUM DYNAMICS OF OPEN QUANTUM SYSTEM 5
Open Quantum System:……6
Example: Thermalized Harmonic Oscillator……9
CHAPTER 3: QUANTIZATION OF LIGHT 10
CHAPTER 4: CAVITY OPTICS 14
CHAPTER 5: INITIAL STATE OF LIGHT AND LIGHT SOURCE 20
CHAPTER 6: OPTICAL CORRELATIONS 24
Second Order Correlation:……27
CHAPTER 7: LIGHT-MATTER INTERACTION 32
One Cavity Mode and One Site:……...32
CHAPTER 8: ONE CAVITY MODE AND TWO SITES 48
Effect of Hopping:……50
Effect of Anharmonicity:……..55
Effect of Resonance:……55
CHAPTER 9: LIGHT HARVESTING COMPLEX II 59
Extension to Full LH-II……69
CHAPTER 10: CONCLUSION AND FUTURE DIRECTION ... 71
BIBLIOGRAPHY 73
APPENDIX 75

LIST OF TABLES

Table 1: The Hamiltonian for two sites and a cavity mode in number basis. Only non-zero values are shown for clarity 48

Table 2: Hopping matrix for site-site excitation exchange 63

LIST OF FIGURES

Figure 1: The conceptual framework for system and environment in an open-quantum-system approach. The system dynamics are dictated by an effective Hamiltonian. 7

Figure 2: Schematic for an optical cavity of length L with fundamental mode inside. 15

Figure 3: Fundamental mode frequency as a function of the wavevector's perpendicular component for an arbitrary cavity with unit length. The speed of light, refractive index of cavity material and the Planck's constant are all consisted 1. 16

Figure 4: A leaky optical cavity with mirror transmission T. Collapse operators couple the mode to the environment. 17

Figure 5: Photon population inside a leaky cavity as a function of time. The cavity starts in 2-photon Fock state and the mirror transmission is 0.25% that gives rise to a leakage rate of 0.0025 fs^{-1}. 18

Figure 6: On left, a cartoon for experimental arrangement of the SPDC process. In the center, a vector diagram for the conservation of momentum and on the right the energy level description of the SPDC. 21

Figure 7: Conceptual cartoon for the experimental setup that utilizes SPDC for producing and pumping 2 photons Fock state in the cavity that contains chromophores (termed sites) interacting with the cavity mode. 22

Figure 8: Detection mechanism for finding the time correlations in the output photon statistics form the optical cavity. 23

Figure 9: Frequency resolved detection setup for the output photons from the optical cavity. 23

Figure 10: The first order correlation along with photon population inside the cavity for a leaky cavity. The blue and yellow curves represent the normalized and non-normalized first order correlations and the green curve shows the photon population inside the cavity. The cavity frequency is at 14716.33 cm^{-1} (hence the rapid oscillation) and the cavity decay rate is 0.0025 fs^{-1}. 26

Figure 11: The frequency spectra for the non-normalized (blue) and normalized (yellow) first order correlations. Both show a single peak at cavity frequency of 14716.33 cm^{-1} with Lorentzian line-shape. 26

Figure 12: Fock state representation of three states of light with $\langle N_{photon} \rangle = 2$. 29

Figure 13: The normalized second order correlation for light leaking from a cavity with initial state as coherent, thermal and Fock states. All have $\langle N_{photon} \rangle = 2$. 30

Figure 14: Non-normalized version of the second order correlation for the photons leaking out of the cavity. 30

Figure 15: Frequency spectrum from non-normalized first order correlation with different states of light inside cavity. 31

Figure 16: Frequency spectrum from normalized first order correlation with different states of light inside cavity. 31

Figure 17: The dispersion relation for upper and lower polaritons for g=30 cm^{-1}. 35

Figure 18: Frequencies for the eigen-energies. The frequencies are shown as a function of the coupling g for the cavity-site system on resonance at 14716 cm^{-1} with $k_{\perp} = 0$. 35

Figure 19: One site and one cavity mode system on resonance with g=30 cm^{-1},$\omega_c=\omega_s=14716.33$ cm^{-1}. With 2 energy units in total, there are 2 sets eigen energies. One is centered on the cavity frequency and the other is centered at twice the cavity frequency. This second set is termed overtones. 37

Figure 20: The dispersion relation for the upper three energy levels for a cavity-site system with 2 units of energy. 37

Figure 21: Cavity-site system with leaky cavity on resonance with site at 14716 cm^{-1}. Each plot shows the evolution of the population for the cavity mode and the site as a function of time for different values of the coupling g. 40

Figure 22: First order correlation for a frequency shifted cavity-site system starting of with 2 photons in the cavity mode. The mirror transmission for the cavity is 0.25 %. As the coupling increases the oscillations increase as well. 41

Figure 23: Frequency spectra associated with single site-cavity model starting in a 2 photon Fock state. The spectra are for different values of coupling showing the fundamental modes of the total system. 42

Figure 24: Second order correlation for the photons leaking out of the cavity for different light-matter couplings. 43

Figure 25: Overtones are shown for one cavity-one site system with 2 photons. The anharmonicity increases the energy for high energy level even higher. The cavity is on resonance with site at ω_c=14716 cm^{-1} and $g = 30$ cm^{-1} 44

Figure 26: The evolution of excitation and photon population with anharmonicity of $u = 50$ cm^{-1}. 45

Figure 27: Effects of the anharmonicity on the first order correlation and frequency spectrum for different coupling strengths. 46

Figure 28: Second order correlation for system with anharmonicity..... 47

Figure 29: Fundamental frequencies and overtones for the 2 sites in a cavity. The light-matter coupling is $g = 30$ cm^{-1}..... 50

Figure 30: Energy level diagram for the eigenvalues of the 2 site-one cavity system with g=30 cm^{-1}, u=0 cm^{-1}, and $t = 36$ cm^{-1}. The presence of hopping energy shifts both the fundamental modes and the overtone. 51

Figure 31: Population dynamics inside the cavity for different values of t with $g = 30$ cm^{-1} and $u = 0$ cm^{-1}. The cavity frequency is $\omega_c = (\omega_{s1}+\omega_{s2})/2$ and $\omega_{s1}<\omega_{s2}$..... 52

Figure 32: First order correlation and spectra for different values of hopping. For this system g=30 cm^{-1} and u=0 cm^{-1}. 53

Figure 33: Photon population in the cavity (top) and second order correlation (bottom) for different values of hopping. For this system g=30 cm^{-1} and u=0 cm^{-1} 54

Figure 34: Population dynamics inside the cavity for different values of t with g=30 cm^{-1} and u=50 cm^{-1}. The cavity frequency is $\omega_c = \omega_{s1}$ and $\omega_{s1}<\omega_{s2}$. 56

Figure 35: Frequency spectrum from first order correlation of photons leaking from cavity. The cavity is on resonance with the frequency of site 1. The coupling and anharmonicity are g=30 cm^{-1} and u=50 cm^{-1}..... 57

Figure 36: Photon population inside the cavity and second order coherence for photons leaking from cavity. The cavity is on resonance with the frequency of site 1. The coupling and anharmonicity are g=30 cm^{-1} and u=50 cm^{-1}..... 58

Figure 37: Monomer structure of LHII complex with 8 chlorophyll a (green) and 6 chlorophyll b (blue). The cholorphylls are numbered from 1 to 14 using 6XX notation for XXth chlorophyll. Only the rings containing the magnesium ions are colored as they are the active sites for these chromophores. The rest of the protein structure that supports these chromophores is shown in gold. The image as been adapted from the work of A. Ishizaki and G. R. Fleming [25]. 60

Figure 38: The chemical structures of chlorophyll a and b. The magnesium ions supported in the ring are the sites where photonic energy is absorbed and converted to excitonic energy in these chromophores. 61

Figure 39: Frequencies for all 14 sites in an LHII monomer. Sites are numbered in ascending order of their frequencies with site 1 at the lowest and site 14 at the highest frequency. 62

Figure 40: Mapping of chromophores to connected lattice graph. The structure of the graph is not related to the actual spatial position of sites in the LHII complex. The vertices are colored according to chromophore type: green for chlorophyll a and blue for chlorophyll b. The thickness of the edges connecting the vertices give indication of the coupling between sites. The vertices are labeled according to their relative site energies with site 1 having the lowest energy and site 14 having the highest. ... 64

Figure 41: Possible states for the LHII monomer in optical cavity. The states are numbered from 0 through 135. The states are in number basis with $\psi = ncavity, nsite1, \dots, nsite14$. The states in red have 2 excitations on a single site, states in yellow have one photon in cavity mode and the last green state has 2 photons in the cavity mode. 65

Figure 42: Population dynamics for the LHII monomer inside the cavity with $\omega_c = (\omega_{s1}+\omega_{s2})/2 = 15136.83$ cm^{-1}. 67

Figure 43: The first order correlation and the associated frequency spectrum for the LHII monomer inside the cavity. 68

Figure 44: The second order correlation for the LHII monomer in the optical cavity. 68

CHAPTER 1: INTRODUCTION

The scientific understanding of the light-matter interaction has been at the heart of the progress in multiple scientific and technical fields. The spectroscopic techniques and insights generated by the study of light-matter interaction have proven to be powerful tools for understanding complex chemical and physical processes in the materials. UV-Vis, Infrared and Raman spectroscopies have provided unique tools for probing electronic, vibrational, and rotational transitions for molecules [1]. X-ray diffractions have opened doors to identification of crystalline structures [2]. Fluorescence and phosphorescence have enabled labeling and tracking of complex chemical and biological mechanisms. Nuclear-Magnetic Resonance (NMR) and Electron spin resonance have especially helped analyze chemical environments for different functional groups in organic compounds. However, in all these spectroscopic methods, the light-matter interaction is treated semi-classically, where the light is a classical electromagnetic radiation and the material is quantum mechanical object with quantized physical properties (such as energy levels and spins). This semiclassical approach overlooks quantum properties of light, hence underutilizing the full features of the interaction. Modeling and utilizing a fully quantum mechanical light-matter interaction for spectroscopic applications can provide new tools, which can access previously unreachable interaction in the material or create alternative routes to classical spectroscopies.

Multiple groups have already started work on the theoretical and experimental fronts for deploying quantum properties of light towards spectroscopy [3-7]. Kalashnikov et al have utilized the quantum interference of entangled photons to measure dephasing time of resonant media on the femto-second timescale using continuous-wave laser and photon coincidence

counting in a modified Hong-Ou-Mandel experiment. This method provides an alternative to traditional experimental setups that require ultrafast-pulsed lasers and sophisticated time-gated optical detection [8]. In another effort, they used the interreference of photons produced in spontaneous parametric down conversion (SPDC) to perform infrared spectroscopy of CO_2 samples using visible light [9]. On the other hand, Mukamel et al have utilized a fully quantum approach to resolve the energy transfer pathways in Light Harvesting Complex II. Their model placed the LHII in an optical cavity to create well-resolved light-matter states called polaritons and utilized multi-dimensional photon coincidence-counting spectroscopy to observe their relaxation dynamics.

Although light can be explained quite well as an oscillating electromagnetic field (that obeys classical Maxwell equations), it does show quantum behavior such as entangled states and photon number states. [10] In the entangled states, the polarizations or frequencies of one photon cannot be observed independently without affecting the state of the other, even when the two are spatially well separated from each other. Similarly, the electromagnetic field associated with light can have quantized energies. This leads to the Number States (Fock States) of light that have well-defined number of photons (this is in stark contrast to classical light, which often shows Planck's distribution) [10, 11]. Upon interacting with quantized material, the quantum light's state gets affected by different processes taking place in the material. Therefore, the quantum state of light becomes a spectroscopic tool for observing the complex processes in the materials.

The experimental apparatus for such experiments often involves an optical cavity since it is a useful apparatus for controlling and modifying properties of light and the light-matter interaction. The material samples placed inside the cavity can interact with a photon far longer

than in free space. Therefore, cavities can enhance light-matter interaction and are particularly suited for experiments with quantum light. The strong interaction of the material samples with the cavity create mixed light-matter states called polaritons. These new states have different energy levels than the original ones. As a result, they can be used to modify the reaction rates for different chemical reactions or eliminate coupling to vibrations [12-14]. Furthermore, the cavity can provide a channel for different parts of the material system to interact with each other even when they are normally disconnected [15-17].

For useful applications, the fully quantum treatment of light matter interaction needs to be carefully modeled to discover effects of different matter-matter interactions on the quantum mechanical state of light and its associated experimental observables. In this work, an optical cavity is considered with LHII complex as sample inside it since LHII complex has been well studied. The material samples are equated to *sites* that can absorb energy in electronics excitations or excitons. A fully quantum model is developed using open system quantum dynamics to model the interaction of light in the cavity mode and the material samples. These models monitor the population dynamics inside the cavity as a function of different intra-material properties. Furthermore, the spectroscopic and statistical properties of the photons leaking from the cavity are studied for identifying the signatures of intra-material processes.

In this thesis, the next two sections discuss the basics of open quantum system approach and the quantization of light, respectively. Afterwards, cavity-optics and mechanism for creating quantum states of light inside the cavity are presented. Then the time-correlations for the photons leaking from the cavity are studied. Subsequent discussions are focused on the light-matter interaction with one and two sites in the cavity. In these systems, the effect of intra-

material and light-matter interactions are explored on the populations inside the cavity and the photons emitted from the cavity. Furthermore, a system of current scientific interest, the LHII complex, is studied in this scheme. Finally, the thesis is concluded with future directions.

CHAPTER 2: QUANTUM DYNAMICS OF OPEN QUANTUM SYSTEM

The time-evolution for the state of an isolated quantum mechanical system follows the Schrodinger equation that is given by

$$i\hbar\frac{\partial}{\partial t}|\psi\rangle = H|\psi\rangle \qquad Eq.(2.1)$$

where $\hbar$ is the Planck's constant and H is the Hamiltonian of the system. If the Planck's constant is taken to be one, the wavefunctions at two different points in time are related by

$$|\psi(t)\rangle = e^{-iH(t-t_0)}|\psi(t_0)\rangle \qquad Eq.(2.2)$$

In Eq. 2.2, the factor $U = e^{-iH(t-t_0)}$ encodes the time-evolution that holds the following property

$$e^{-iH(t-t_0)} = e^{-iH(t-t_i)}e^{-iH(t_i-t_0)} \text{ for } t_0 < t_i < t$$

Since the Hamiltonian is a Hermitian operator ($H = H^\dagger$), the operator U is unitary ($U^\dagger U = UU^\dagger = I$) and the evolution is reversible. Therefore, the time-evolution does not change the norm of the state vector i.e.

$$\frac{\partial}{\partial t}\langle\psi|\psi\rangle = 0 \qquad Eq.(2.3)$$

More generally, the state of a quantum system can be represented by the density matrix ρ, which is related to the state vector by

$$\rho = |\psi\rangle\langle\psi|$$

Using the density matrix, the time-evolution is given by

$$i\hbar\frac{\partial}{\partial t}\rho = [H,\rho] \qquad Eq.(2.4)$$

The solution for this differential equation (Eq. 2.4) gives the following expression

$$\rho(t) = e^{-iH(t)}\rho_0 e^{+iH(t)} \qquad Eq.(2.5)$$

here $\hbar = 1$, $t_0 = 0$ and $\rho_0 = \rho(0)$.

The density matrix further shows the following properties:

1. $tr(\rho) = 1$
2. ρ is Hermatian: $\rho = \rho^{\dagger}$
3. The eigenvalues of the density matrix (i.e. ρ_n) are real and $0 \leq \rho_n \leq 1$.

Therefore, the eigenvalues of ρ can be interpreted as probabilities for the system being in the corresponding eigenstates.

Open Quantum System:

An isolated quantum system is an ideal scenario. In reality, the system is often connected to the environment through multiple different types of interactions (Figure 1). These interactions can lead to an irreversible process. The effective Hamiltonian describing an irreversible process is non-Hermitian. If the effective Hamiltonian is time-independent, it can be give by

$$H_{eff} = H_0 - iV \qquad Eq.(2.6)$$

here H_0 and V are Hermitian making iV anti-Hermitian. As a result, if V is absent, the system's evolution becomes reversible.

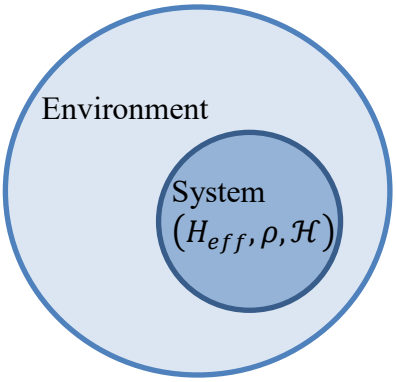

Figure 1: The conceptual framework for system and environment in an open-quantum-system approach. The system dynamics are dictated by an effective Hamiltonian.

The time-evolution generated by H_{eff} leads to an exponential decay or growth of the wavefunction amplitude such that

$$\frac{\partial}{\partial t}\langle\psi|\psi\rangle = -2\langle\psi|V|\psi\rangle \qquad Eq.(2.7)$$

Since the wavefunction represents a physical system throughout the time-evolution, $\langle\psi|\psi\rangle \leq 1$, and

$$\langle\psi|V|\psi\rangle \geq 0 \qquad Eq.(2.8)$$

Since V is Hermitian, it can be rewritten as $V = \gamma T^{\dagger}T$, leading to

$$\langle\psi|V|\psi\rangle = \gamma\langle\psi|T^{\dagger}T|\psi\rangle = \left(\sqrt{\gamma}\,T|\psi\rangle\right)^{\dagger}\left(\sqrt{\gamma}\,T|\psi\rangle\right) \qquad Eq.(2.9)$$

Additionally, if $|\alpha\rangle$ represent the eigenvectors of V with eigenvalues V_α then

$$V = \sum_{\alpha} V_\alpha\,|\alpha\rangle\langle\alpha| \qquad Eq.(2.10)$$

Since $\langle\psi|V|\psi\rangle \geq 0$, the eigenvalues are non-negative. A comparison of the two expressions for V concludes that $V_\alpha = \gamma_\alpha$ and $|\alpha\rangle\langle\alpha| = T_\alpha$ such that $T = \sum T_\alpha$. The operators T_α describe sub-processes that are irreversible and γ_α are the rates of these sub processes.

The Hamiltonian dynamics discussed so far only accounts for the probability to stay in a quantum state. However, the system can also undergo stochastic changes such as quantum jumps (or collapse of the wavefunction) which occur with probability $1 - \langle\psi|\psi\rangle$. The mathematical action of the quantum-jump process on a state or density matrix can be given by

$$|\psi\rangle \rightarrow \mathcal{J}_\alpha |\psi\rangle$$

$$\rho \rightarrow \mathcal{J}_\alpha \rho \mathcal{J}_\alpha^\dagger$$

where $\mathcal{J}_\alpha$ is the jump operator from the irreversible processes that constitute the system-environment coupling. Under the action of both the dissipation and the quantum jumps, the dynamics is given by

$$\frac{\partial \rho}{\partial t} = i[\rho, H_{eff}] + \sum\nolimits_\alpha \Gamma_\alpha \mathcal{J}_\alpha \rho \mathcal{J}_\alpha^\dagger \qquad Eq.(2.11)$$

where Γ_α is the rate for a given quantum jump process. If the total probability over all possible states for the quantum system is preserved then trace of density matrix should not change over system evolution since it gives the sum-total of all probabilities

$$\frac{\partial}{\partial t} tr(\rho) = 0 = \sum\nolimits_\alpha \left(-2\gamma_\alpha T_\alpha \rho T_\alpha^\dagger\right)\left(\Gamma_\alpha \mathcal{J}_\alpha \rho \mathcal{J}_\alpha^\dagger\right) \qquad Eq.(2.12)$$

This generates the following relations

$$2\gamma_\alpha = \Gamma_\alpha$$

$$T_\alpha = \mathcal{J}_\alpha$$

Substituting these results in Eq. 2.11gives

$$\frac{\partial \rho}{\partial t} = i[\rho, H_{eff}] + \sum\nolimits_\alpha 2\gamma_\alpha T_\alpha \rho T_\alpha^\dagger$$

$$\frac{\partial \rho}{\partial t} = i[\rho, H_0] + \sum\nolimits_\alpha \gamma_\alpha \left(-T_\alpha^\dagger T_\alpha \rho + 2T_\alpha \rho T_\alpha^\dagger - \rho T_\alpha^\dagger T_\alpha\right) \qquad Eq.(2.13)$$

Eq. 2.13 is known as the Lindblad equation that governs the evolution of quantum systems with dissipative dynamics [18]. The first part on the right generate the non-dissipative evolution. The second part generates dissipative evolution of the density matrix due to interaction of the system with the environment through operators T_α and with rates γ_α for sub-processes α.

Example: Thermalized Harmonic Oscillator

A quantum Harmonic oscillator with frequency ω is defined by the following Hamiltonian

$$H = \hbar\omega a^\dagger a$$

If it is connected to a thermal bath, the excitations are lost and acquired through the jump or collapse operators $\sqrt{\gamma_1}a$ and $\sqrt{\gamma_2}a^\dagger$, respectively. Let the average thermal excitations at the bath temperature be $\langle n_{th}\rangle$ and the coupling between the oscillator and bath be κ, then the following process are possible

1. Lost or gain of thermal excitation with rate $\kappa\langle n_{th}\rangle$
2. Lost of harmonic oscillator's excitation to the bath at rate κ

The detailed balance then requires

$$\gamma_1 = \kappa(1 + \langle n_{th}\rangle)$$

$$\gamma_2 = \kappa\langle n_{th}\rangle$$

Therefore, the corresponding Lindblad equation becomes

$$\frac{\partial\rho}{\partial t} = i\hbar\omega[\rho, a^\dagger a] + \gamma_1(-a^\dagger a\rho + 2a\rho a^\dagger - \rho a^\dagger a) + \gamma_2(-aa^\dagger\rho + 2a^\dagger\rho a - \rho aa^\dagger)$$

CHAPTER 3: QUANTIZATION OF LIGHT

The fundamental relations governing the behavior of an electromagnetic radiation (light) are encapsulated in Maxwell's equations (Eq. 3.1-3.4). Using Gaussian units and Columb-guage, the Maxwell's equation for free-space are

$$\boldsymbol{\nabla}.\boldsymbol{E} = 0 \qquad Eq.(3.1)$$

$$\boldsymbol{\nabla}.\boldsymbol{B} = 0 \qquad Eq.(3.2)$$

$$\boldsymbol{\nabla} \times \boldsymbol{E} = -\frac{1}{c}\frac{\partial \boldsymbol{B}}{\partial t} \qquad Eq.(3.3)$$

$$\boldsymbol{\nabla} \times \boldsymbol{B} = -\frac{1}{c}\frac{\partial \boldsymbol{E}}{\partial t} \qquad Eq.(3.4)$$

where $\boldsymbol{B} = \boldsymbol{\nabla} \times \boldsymbol{A}$ is the magnetic induction and $\boldsymbol{E} = \left(-\frac{1}{c}\frac{\partial \boldsymbol{A}}{\partial t} - \boldsymbol{\nabla}\phi\right)$, is the electric field with ϕ and A representing the scalar and vector potentials, respectively [19]. In these equations, c is the speed of light and the space is considered free of any charge or current. These relations lead to the following wave equation for light:

$$\nabla^2 \boldsymbol{A} - \frac{1}{c^2}\frac{\partial^2 \boldsymbol{A}}{\partial t^2} = 0 \qquad Eq.(3.5)$$

A possible solution for this wave equation is a monochromatic (single frequency) plane wave.

$$\boldsymbol{A}(\boldsymbol{r}, t) = \alpha(t)\boldsymbol{A_0}(\boldsymbol{r}) + \alpha^*(t)\boldsymbol{A_0^*}(\boldsymbol{r}) \qquad Eq.(3.6)$$

with $\alpha(t) = \alpha(0)e^{-i\omega t}$ and $\boldsymbol{A_0}(\boldsymbol{r})$ that satisfy

$$\nabla^2 \boldsymbol{A_0}(\boldsymbol{r}) + k^2 \boldsymbol{A_0}(\boldsymbol{r}) = 0 \quad \left(k = \frac{\omega}{c}\right)$$

The corresponding electric and magnetic fields are given by

$$\boldsymbol{E}(\boldsymbol{r}, t) = -\frac{1}{c}\left(\dot{\alpha}(t)\boldsymbol{A_0}(\boldsymbol{r}) + \dot{\alpha}^*(t)\boldsymbol{A_0^*}(\boldsymbol{r})\right) \qquad \text{Eq. (3.7)}$$

$$\boldsymbol{B}(\boldsymbol{r}, t) = \alpha(t)\boldsymbol{\nabla} \times \boldsymbol{A_0}(\boldsymbol{r}) + \alpha^*(t)\boldsymbol{\nabla} \times \boldsymbol{A_0^*}(\boldsymbol{r}) \qquad Eq.(3.8)$$

From equation 3.7 and 3.8, it is inferred that the spatial variation of the electric and the magnetic fields is dictated by $\boldsymbol{A}$**,** whereas the temporal evolution of the two fields is encoded in α [20]. The energy contained in this electromagnetic field and hence its classical Hamiltonian is given by

$$H_{field} = \frac{1}{8\pi} \int d^3r(\boldsymbol{E}^2 + \boldsymbol{B}^2) = \frac{k^2}{2\pi}|\alpha(t)|^2 \qquad Eq.(3.9)$$

Therefore, the electromagnetic field of light is equivalent to a classical harmonic oscillator Hamiltonian given by

$$H = \frac{1}{2}(p^2 + \omega^2 q^2) \qquad Eq.(3.10)$$

for $q(t) = \frac{i}{c\sqrt{4\pi}}[\alpha(t) - \alpha^*(t)]$ and $p(t) = \frac{k}{\sqrt{4\pi}}[\alpha(t) + \alpha^*(t)]$

Consequently, the procedure of quantizing light is similar to the procedure of quantizing a harmonic oscillator, resulting in

$$H_{field} = \hbar\omega\left(a^\dagger a + \frac{1}{2}\right) \qquad Eq.(3.11)$$

$$a = \sqrt{\frac{\omega}{2\pi\hbar c^2}}\ \alpha(t) \qquad Eq.(3.12)$$

$$a^\dagger = \sqrt{\frac{\omega}{2\pi\hbar c^2}}\ \alpha^*(t) \qquad Eq.(3.13)$$

$$[a, a^\dagger] = 1 \qquad Eq.(3.14)$$

where a and $a^\dagger$ are lowering and raising operators that are related to α, the time evolution of light. In case of a medium with refractive index η, the speed of light in these equations will be replaced by $\frac{c}{\eta}$.

The relation of the electric and magnetic fields to the raising operators is

$$E(r,t) = i\sqrt{2\pi\hbar\omega}\,\left(a(t)A_0(r) - a^{\dagger}(t)A_0^{*}(r)\right) \qquad Eq.(3.15)$$

$$B(r,t) = \sqrt{\frac{2\pi\hbar c^2}{\omega}}\left(a(t)\left(\nabla \times A_0(r)\right) + a^{\dagger}(t)\left(\nabla \times A_0^{*}(r)\right)\right) \qquad Eq.(3.16)$$

The eigenstates of the light mode are called number states $|n\rangle$, which contain a precise number of quanta and the action of the raising or lowering operator is defined by:

$$a|n\rangle = \sqrt{n}|n-1\rangle \qquad Eq.(3.17)$$

$$a^{\dagger}|n\rangle = \sqrt{n+1}|n+1\rangle \qquad Eq.(3.18)$$

The intensity of classical light is described by the square of the electric field, in quantum version the expectation value of intensity leads to:

$$\langle \boldsymbol{E}^2(\boldsymbol{r},t)\rangle = \; 4\pi\hbar\omega|\boldsymbol{A_0}(\boldsymbol{r})|^2\, n + \langle \boldsymbol{E}^2(\boldsymbol{r})\rangle_0 \qquad Eq.(3.19)$$

The first term on the right shows that the spatial variation of the quantized electric field is same as that of the classical field i.e. $\boldsymbol{A_0}(\boldsymbol{r})$; however, the temporal variation has now been quantized into n. Consequently, if the electric field for the classical light is zero at some point in space for all times (for example a node); the quantum version will also show zero probability for a photon at those places. The factor n is the number of photons in the field whose spatial variation is exactly same as that of the classical light.

This technique can be extended to electric field containing multiple modes such as light in free space and the quantization can be performed in the reciprocal k-space. The resulting Hamiltonian is given by

$$H_{field} = \sum_{\boldsymbol{k}\lambda} \hbar\omega_{\boldsymbol{k}}\left(a^{\dagger}_{\boldsymbol{k}\lambda}a_{\boldsymbol{k}\lambda} + \frac{1}{2}\right) \qquad Eq.(3.20)$$

where λ is the wavelength of light, $\boldsymbol{k}$ is the wavevector, and the summation runs over all possible values. The wave vector is related to the frequency by:

$$\omega_k = c|k| \text{ and } |k| = \frac{1}{\lambda}$$

Here c is the speed of light. The commutation relations between different raising and lowering operators follow:

$$\left[a_{\boldsymbol{k}\lambda}(t), a^{\dagger}_{\boldsymbol{k}'\lambda'}(t)\right] = \delta^3_{\boldsymbol{k},\boldsymbol{k}'}\delta_{\lambda} \qquad Eq.(3.21)$$

This indicates that the light modes obey bosonic statistics, which implies that multiple particles of light (called *photons*) can occupy the same state. It is worth remembering at this point that a number state $|n\rangle$ contains n photons in the same state, a situation that would not be possible if the photons were not bosonic.

CHAPTER 4: CAVITY OPTICS

An optical cavity presents an interesting test ground for exploring and controlling light-matter interaction. These special electromagnetic conditions inside the cavity give rise to interesting phenomenon such as Casimir Effect and modified light-matter interaction. The modified interactions can lead to the enhancement or reduction of the excited-state lifetime for matter. Furthermore, a photon of light in free space would possibly interact only once with an atom; however, in an optical cavity the interaction can be repeated multiple times. Therefore, cavity can assist in probing intra-material interactions through light.

Modern optical cavities are often fabricated by depositing layers of different materials with carefully selected refractive indices and thicknesses. However, conceptually an optical cavity is equivalent to a pair of mirrors separated by a distance L as shown in Figure 2. The electric field in-between the mirrors can exist only in certain modes dictated by the boundary conditions on Maxwell equations and the wave equation for light. These modes are commonly termed cavity-modes. The restrictions placed by this mode structure allows only a select set of wavelengths along the length of the cavity. Any different wavelength light will be unstable inside the cavity. For a mode along the length of the cavity, the relationship between the mode-wavelength and the cavity length is encapsulated by the following equation.

$$\lambda_m = \frac{2L}{m} \; for \; m \in [1, 2, 3, \dots \;]$$

where m is the mode number.

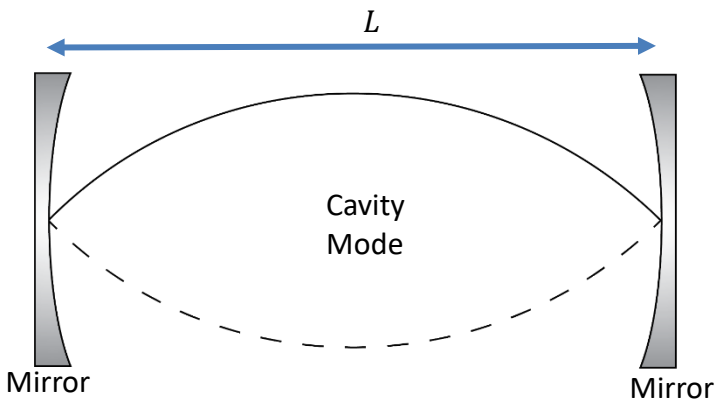

Figure 2: Schematic for an optical cavity of length L with fundamental mode inside.

More generally, the cavity mode can be represented by the wave-vector

$$\boldsymbol{k} = \boldsymbol{k}_{\perp} + \boldsymbol{k}_{\parallel}$$

Here the k vector has been separated into a component that is parallel to the length of the cavity and another that is perpendicular to the cavity axis. The cavity modes only restrict the parallel component; however, the perpendicular component can change continuously. In contrast, both components are continuously variable for light in free space. The relationship between the mode energy and wavevector is

$$\hbar\omega_{k,m} = \frac{\hbar c}{\eta}\sqrt{k_{\perp}^2 + \left(\frac{m}{2L}\right)^2} \qquad Eq.(4.1)$$

Where η is the refractive index of the cavity medium. Since the main focus of this research endeavor is the study of LH-II complex, this relation has been graphically represented in Figure 3 for a cavity with a fundamental mode frequency of $14716.33\ cm^{-1}$ (at $\boldsymbol{k}_{\perp} = 0$) that is resonant with the lowest energy chromophore in LH-II complex. The refractive index for this cavity is $\eta = 1$. The graph shows that energy curves smoothly near $\boldsymbol{k}_{\perp} = 0$ however for large values of $\boldsymbol{k}_{\perp}$ the relationship is linear.

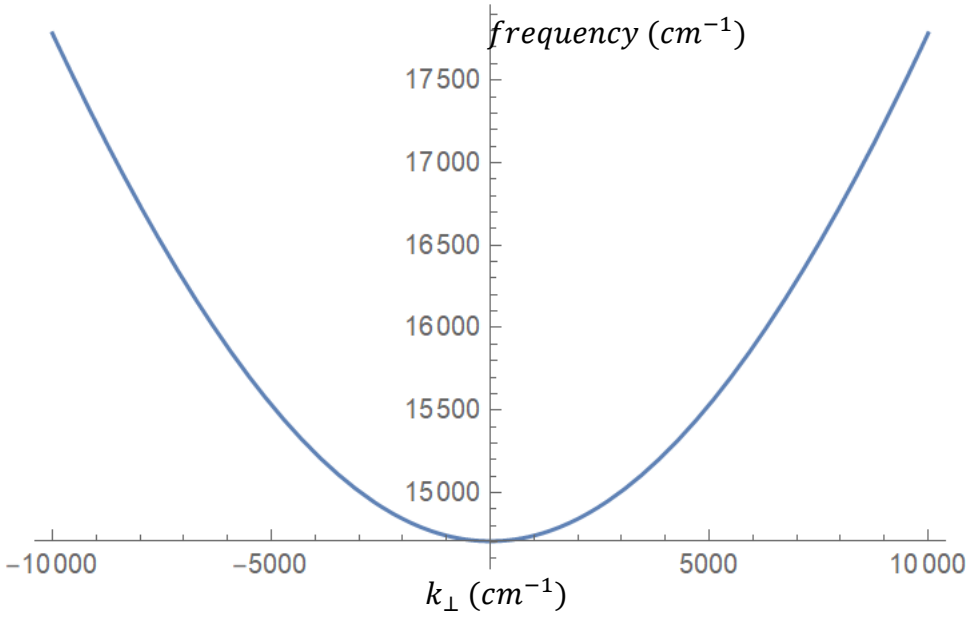

Figure 3: Fundamental mode frequency as a function of the wavevector's perpendicular component for an arbitrary cavity with unit length. The speed of light, refractive index of cavity material and the Planck's constant are all consisted 1.

Practically the cavity mirrors are imperfect, leading to leakage of light into and out of the cavity. If the transmission of the cavity mirrors is t, the cavity Hamiltonian and the collapse operators for the leakage/pumping are given by

$$H_{cavity} = \sum_k \hbar\omega_k a_k^\dagger a_k \qquad Eq.(4.2)$$

$$T_k = \sqrt{t}\, a_k \qquad Eq.(4.3)$$

$$T_k^\dagger = \sqrt{t}\, a_k^\dagger \qquad Eq.(4.4)$$

If only the fundamental mode of cavity is considered through experimental selection, the above expressions reduce down to

$$H_{cavity} = \hbar\omega_0 a_0^\dagger a_0 \qquad Eq.(4.5)$$

$$T_{leak} = \sqrt{t}\, a_0 \qquad Eq.(4.6)$$

$$T_{pump}^\dagger = \sqrt{t}\, a_0^\dagger \qquad Eq.(4.7)$$

Without consistent pumping, the equation of motion for the lowering operator of cavity mode starting with some photons in it is given by

$$i\hbar\frac{\partial\hat{a}}{\partial t} = \hbar\omega_0\hat{a} - i\gamma\hat{a} \qquad Eq.(4.8)$$

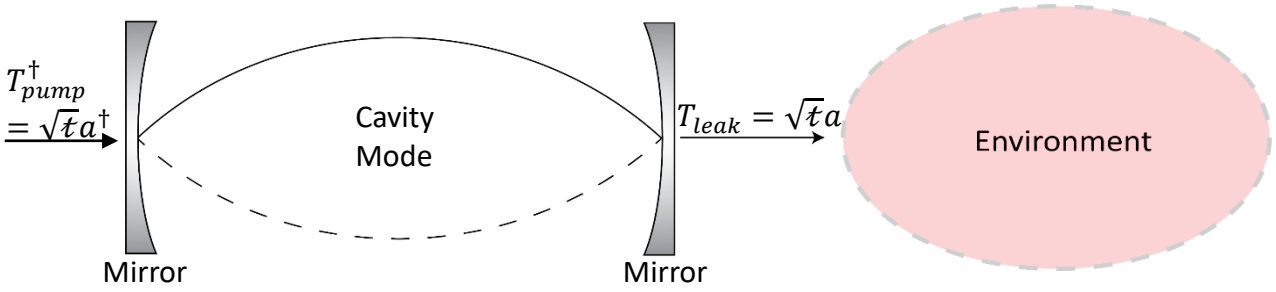

Figure 4: A leaky optical cavity with mirror transmission T. Collapse operators couple the mode to the environment.

In Figure 6, the evolution of the expectation value for number of photons in a leaky cavity starting with 2 photons ($|n\rangle = |2\rangle$) is shown. The cavity frequency is on resonant with the lowest energy chromophore of the LH-II complex. Here the transmission of the cavity mirrors is 0.25% that results in a leakage and the population decays over time. The cavity frequency is $14716\ cm^{-1}$ for the fundamental mode with $\boldsymbol{k}_{\perp} = 0$; therefore, the corresponding cavity length is $\sim 340\ nm$.

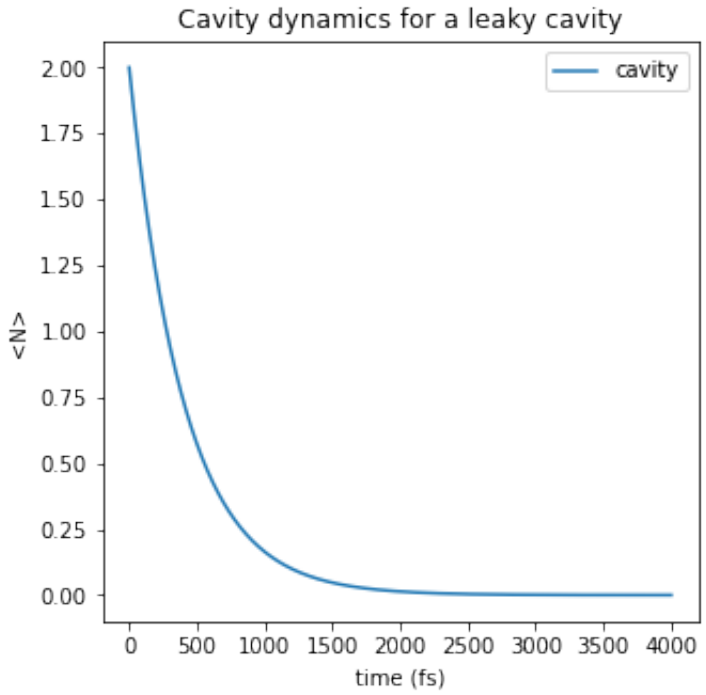

Figure 5: Photon population inside a leaky cavity as a function of time. The cavity starts in 2-photon Fock state and the mirror transmission is 0.25% that gives rise to a leakage rate of 0.0025 fs^{-1}.

The photon population follows an exponential decay. The profile is given by

$$N(t) = N_0 e^{-\gamma t} \qquad Eq.(4.9)$$

where, N is the population of photons inside the cavity and the decay rate is $\gamma = 0.0025\ fs^{-1}$. The half-life of the photon population is ~277 fs which implies that the a photon would virtually make 244 traverses of the cavity length.

If a material sample of interest is placed inside the cavity, the average time spent by the photon inside the cavity will affect the light-matter interaction. Therefore, if the leakage rate is small, the photon will interact with the material sample longer and lead to more pronounced effects on the dynamics of the system. A prolonged photon presence inside the cavity can give

rise to mixed states of light and matter named *polaritons*. The polaritons are hybrid particles that are made of a photon strongly coupled to a material excitation.

CHAPTER 5: INITIAL STATE OF LIGHT AND LIGHT SOURCE

The coherent and thermal states with 2-photons photons on average require 10 to 15 Fock basis for an accurate representation [19]. However, a Fock state only requires one. Therefore, computationally it is more feasible to simulate large photon states for Fock state than for coherent or thermal states. In interacting quantum systems, the dimensionality (and hence the size) of the total Hilbert-space increases exponentially with the increase in number of basis for the subsystems. Consequently, for this work the initial state of light is considered a 2-photon Fock state.

To generate an accurate 2-photon Fock state experimentally, a spontaneous parametric down-conversion (SPDC) process can be used. In an SPDC process, a high energy photon is converted into two low energy photons using a special non-linear crystal [21]. The conversion process follows the conservation of energy and momentum. The original photon is typically called *pump* and the two new photons are called *signal* and *idler*. The conservation of energy implies

$$\omega_{pump} = \omega_{signal} + \omega_{idler}$$

The phenomenological description for this process is given in Figure 7. The pump excites the SPDC crystal to a virtual state from where it falls back to the ground state by emitting the signal and idler photons.

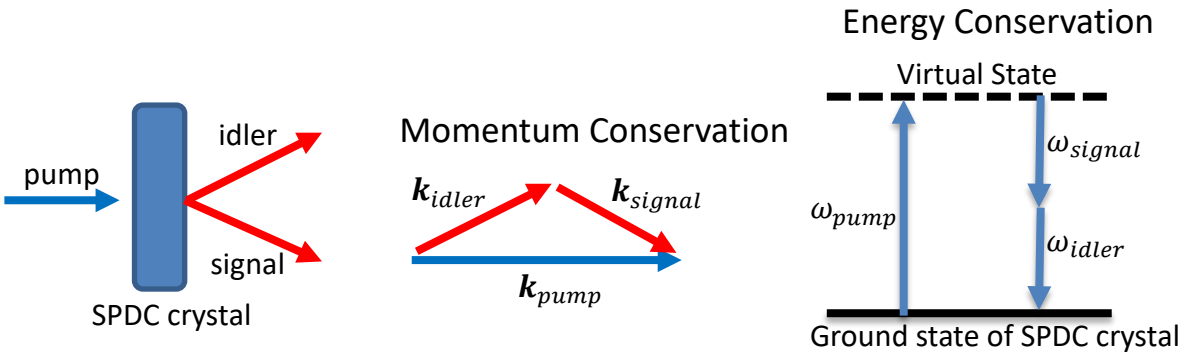

Figure 6: On left, a cartoon for experimental arrangement of the SPDC process. In the center, a vector diagram for the conservation of momentum and on the right the energy level description of the SPDC.

Experimental conditions can be adjusted to generate both the signal and idler photons at the cavity frequency. In terms of Fock state representation, the SPDC process can be described as

$$|\psi_{pump}\rangle \rightarrow \sum_{n} |n_{signal}, n_{idler}\rangle$$

If the pump intensity is low enough, the output state from the SPDC process can be $|1,1\rangle$. This is the required 2-photon state because the cavity dynamics do not differentiate between the signal or idler photons. These photons can be directed into the cavity to generate a 2-photon Fock state inside the cavity. The cartoon of this process is depicted in Figure 8 where materials of interest have been introduced in the cavity as *sites*. Such sites can be chromophores that can interact with the cavity mode and store energy in electronic excitations.

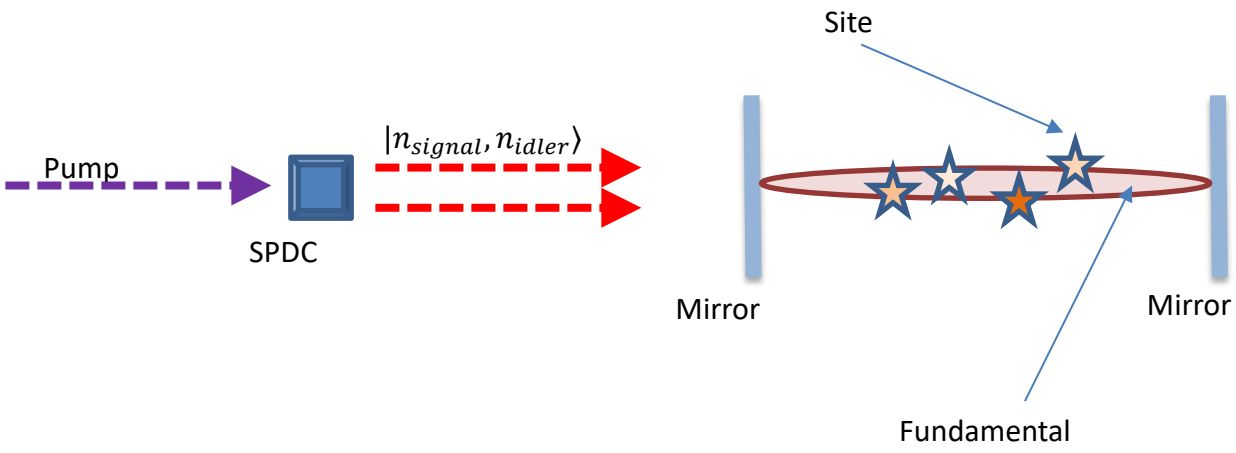

Figure 7: Conceptual cartoon for the experimental setup that utilizes SPDC for producing and pumping 2 photons Fock state in the cavity that contains chromophores (termed sites) interacting with the cavity mode.

A pulsed pump beam can be used to mark and control the time at which the 2-photon Fock state is created. The simplest situation where the cavity starts with 2 photon Fock state and dissipates energy without pumping, can be achieved by decreasing the pulse rate for the pump beam such that a new pair of photons enters the cavity only after the old one has completely leaked out.

The presence of interacting chromophores or sites inside the cavity gives rise to light-matter mixed states. The discussion on this interaction is delayed to later chapters.

The photons leaking from the fundamental mode of the cavity at $\boldsymbol{k}_{\perp} = 0$ can be measured with a time-resolved photo-detector placed along the axis of the cavity. The conceptual framework for the setup is shown in Figure 9. The measurements from such detection scheme can be used to compute the different temporal correlations in the photon statistics. Detailed description of these correlations and their connections to the cavity dynamics are discussed in the following chapter. Furthermore, the spectrum can be acquired either by the Fourier transform of the first order correlation or by a frequency sensitive detection mechanism such

as the one shown in Figure 10. Here a diffraction grating is utilized to resolve different frequencies present in the output light and each frequency is directed to a spatially unique position, where a unique photon detector records the signal (photon).

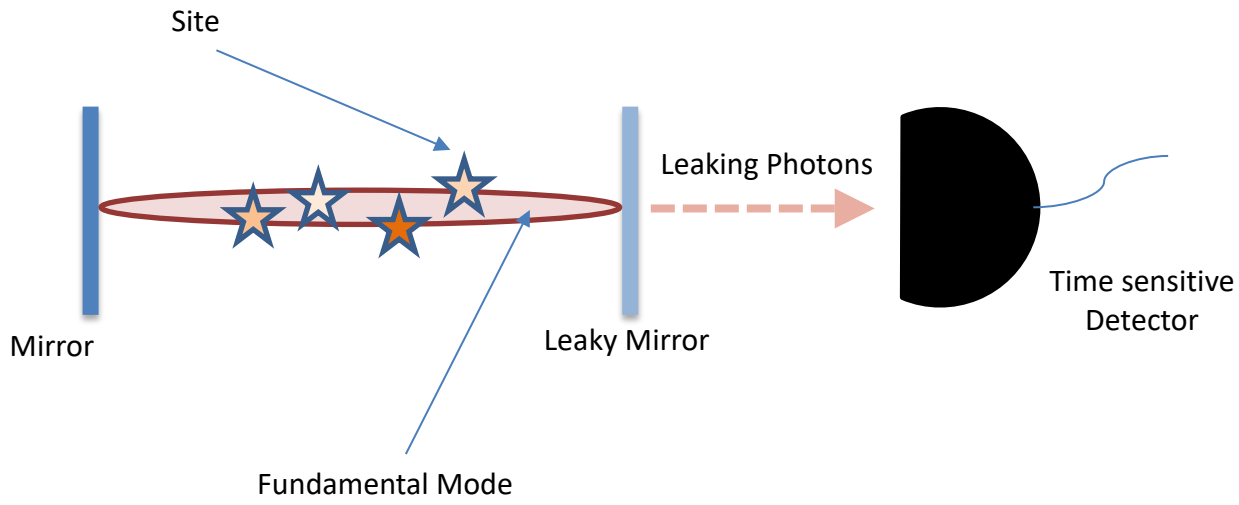

Figure 8: Detection mechanism for finding the time correlations in the output photon statistics form the optical cavity.

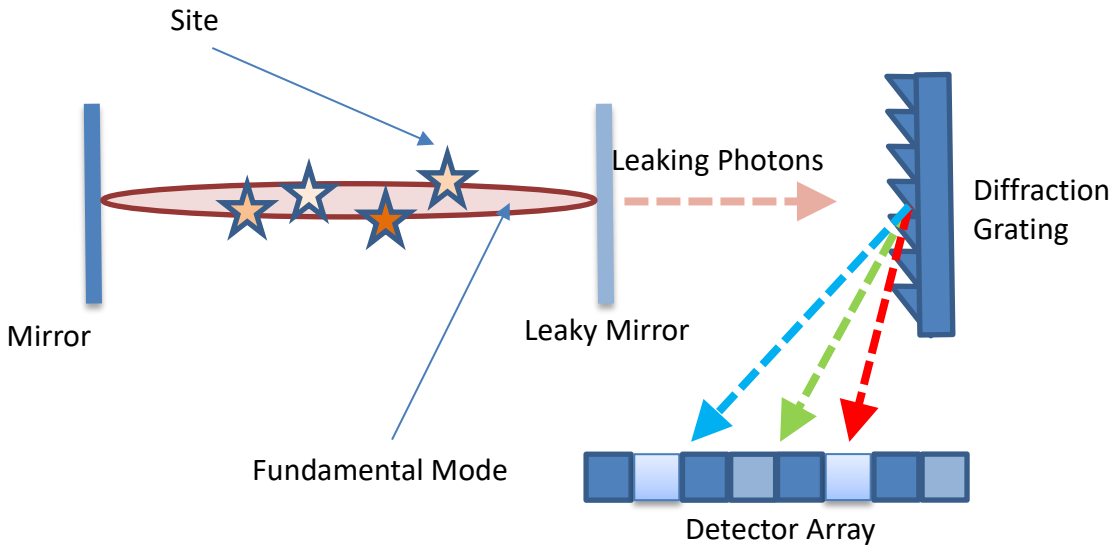

Figure 9: Frequency resolved detection setup for the output photons from the optical cavity.

CHAPTER 6: OPTICAL CORRELATIONS

Although the expectation value of the photon number operator inside the cavity is an observable that can be monitored in simulations, but it is not an experimentally feasible observable. Most experiments rely on detecting leaked photons outside the cavity with time and/or frequency sensitive detectors. Therefore, experimentally the observables that are more useful are those that are associated to these leaked photons. The two commonly studied observables are the first and second order correlations termed $g^{(1)}(\tau)$ and $g^{(2)}(\tau)$, respectively.

Classically, the first order correlation for light captures the fluctuations in the electric field associated with light. Therefore, it is an amplitude-amplitude correlation between two points in space and time. It is given by

$$G^{(1)}(\boldsymbol{r_1}, t_1; \boldsymbol{r_2}, t_2) = \langle E^*(\boldsymbol{r_1}, t_1) E(\boldsymbol{r_2}, t_2) \rangle \qquad Eq.(6.1)$$

where t and $\boldsymbol{r}$ are time and position, respectively [19]. The $\langle\rangle$ represent space and time average over the wavefunction. To remove any artifacts introduced by the increase or decrease in the overall intensity of light, it is often normalized such that

$$g^{(1)}(\boldsymbol{r_1}, t_1; \boldsymbol{r_2}, t_2) = \frac{\langle E^*(\boldsymbol{r_1}, t_1) E(\boldsymbol{r_2}, t_2) \rangle}{\sqrt{\langle |E(\boldsymbol{r_1}, t_1)|^2 \rangle \langle |E(\boldsymbol{r_2}, t_2)|^2 \rangle}} \qquad Eq.(6.2)$$

If the measurements are performed at same point in space but different points in time separated by a delay τ, the above expression can be simplified to

$$g^{(1)}(\tau) = \frac{\langle E^*(t) E(t+\tau) \rangle}{\sqrt{\langle |E(t)|^2 \rangle \langle |E(t+\tau)|^2 \rangle}} \qquad Eq.(6.3)$$

For quantized light, the electric field can be replaced by the raising and lowering operators. Therefore, the first order correlation becomes

$$g^{(1)}(\tau) = \frac{\langle a^{\dagger}(t)a(t+\tau)\rangle}{\sqrt{\langle a^{\dagger}(t)a(t)\rangle\langle a^{\dagger}(t+\tau)a(t+\tau)\rangle}} \qquad Eq.(6.4)$$

For the system under study, the cavity starts with 2 photons at time $t = 0$ and before that the cavity is considered empty; the time t can be fixed at zero. This leads to

$$g^{(1)}(\tau) = \frac{\langle a^{\dagger}(0)a(\tau)\rangle}{\sqrt{\langle n(0)\rangle\langle n(\tau)\rangle}} \qquad Eq.(6.5)$$

$$G^{(1)}(\tau) = \langle a^{\dagger}(0)a(\tau)\rangle \qquad Eq.(6.6)$$

where $n = a^{\dagger}a$ is the photon number operator. On the other hand if there is a steady state photon population inside the cavity (via pumping), any value for t can be set to zero. For monochromatic light outside the cavity with frequency ω, the wavefunctions are represented by plane waves and the $g^{(1)}(\tau)$ becomes

$$g^{(1)}(\tau) = e^{-i\omega\tau} \qquad Eq.(6.7)$$

The Fourier transform of $g^{(1)}$ gives the power spectrum of the light leaking out of the cavity; therefore, for monochromatic light, a single frequency ω will be observed. Consequently, the experimental measurements can be performed either with a time sensitive photo-detector or with a frequency sensitive spectrograph.

For a leaky cavity presented earlier, the non-normalized and normalized first order correlations are presented in Figure 11 along with the cavity's photon population. The rapid oscillations observed in both $g^{(1)}$ and $G^{(1)}$ are at the cavity frequency of $14716.33\ cm^{-1}$. Additionally, $G^{(1)}$ shows an exponential-decay envelop that is dictated by the photon population of the cavity. When $G^{(1)}$ is normalized with exponentially decaying population (green line in Figure 11), the exponential decay envelop is removed. Similar $g^{(1)}$ will be obtained if the population inside the cavity is kept constant through additional pumping.

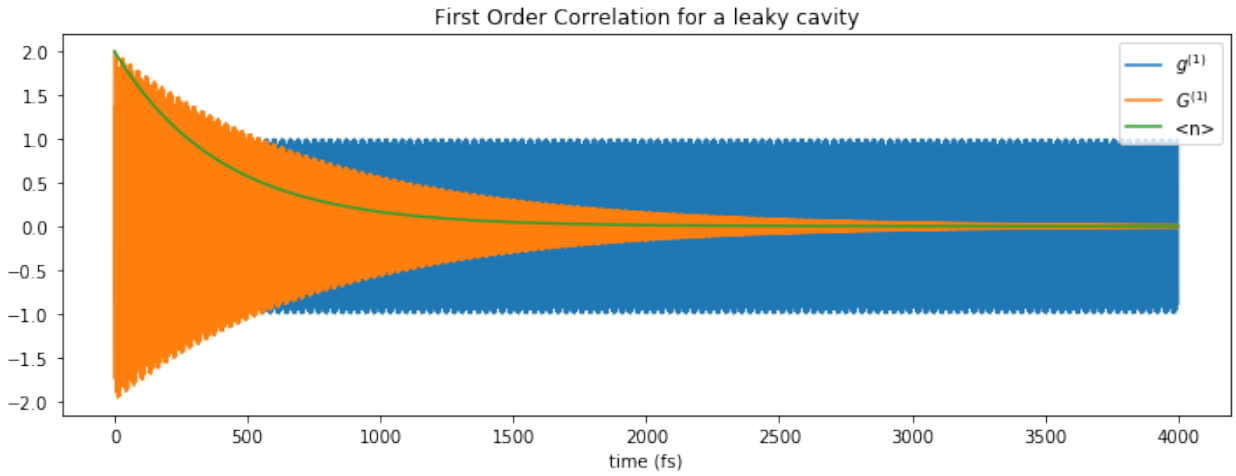

Figure 10: The first order correlation along with photon population inside the cavity for a leaky cavity. The blue and yellow curves represent the normalized and non-normalized first order correlations and the green curve shows the photon population inside the cavity. The cavity frequency is at 14716.33 cm^{-1} (hence the rapid oscillation) and the cavity decay rate is 0.0025 fs^{-1}.

The frequency spectra for both $g^{(1)}$ and $G^{(1)}$ show the cavity frequency. The spectrum shows a Lorentzian line-shape with the line-width dictated by the photon decay rate (Figure 12).

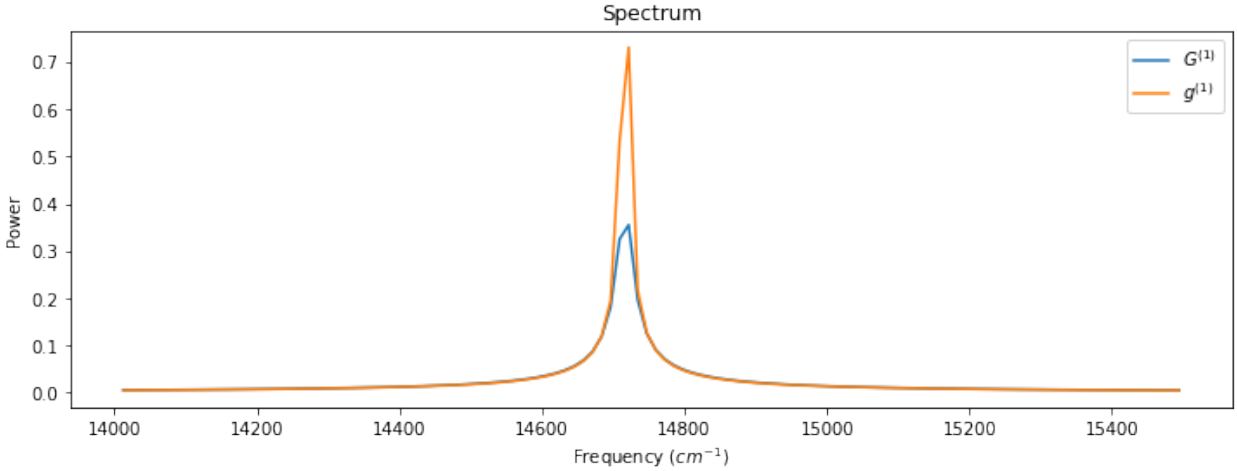

Figure 11: The frequency spectra for the non-normalized (blue) and normalized (yellow) first order correlations. Both show a single peak at cavity frequency of 14716.33 cm^{-1} with Lorentzian line-shape.

The energy level of the system can be shifted without introducing any artifacts. Therefore, down-shifting cavity energy by $14716\ cm^{-1}$ to $0.33\ cm^{-1}$ can remove the fast oscillating terms from the $g^{(1)}$.

Second Order Correlation:

Classically, the second order correlation and its normalized versions are given by

$$G^{(2)}(\boldsymbol{r_1}, t_1; \boldsymbol{r_2}, t_2) = \langle E^*(\boldsymbol{r_1}, t_1) E^*(\boldsymbol{r_2}, t_2) E(\boldsymbol{r_1}, t_1) E(\boldsymbol{r_2}, t_2) \rangle \qquad Eq.(6.8)$$

$$g^{(2)}(\boldsymbol{r_1}, t_1; \boldsymbol{r_2}, t_2) = \frac{\langle E^*(\boldsymbol{r_1}, t_1) E^*(\boldsymbol{r_2}, t_2) E(\boldsymbol{r_1}, t_1) E(\boldsymbol{r_2}, t_2) \rangle}{\langle |E(\boldsymbol{r_1}, t_1)|^2 \rangle \langle |E(\boldsymbol{r_2}, t_2)|^2 \rangle} \qquad Eq.(6.9)$$

With the same assumptions as the ones made for first order correlations, the second order correlation can be reduced to

$$g^{(2)}(\tau) = \frac{\langle I(t) I(t+\tau) \rangle}{\langle I(t) \rangle^2} \qquad Eq.(6.10)$$

where $I = E^* E$ is the intensity of light. For quantized light the expressions are

$$g^{(2)}(\tau) = \frac{\langle a^\dagger(t) a^\dagger(t+\tau) a(t+\tau) a(t) \rangle}{\langle a^\dagger(t) a(t) \rangle^2} \qquad Eq.(6.11)$$

$$G^{(2)}(\tau) = \langle a^\dagger(t) a^\dagger(t+\tau) a(t+\tau) a(t) \rangle \qquad Eq.(6.12)$$

and once again, the t can be fixed to zero [19].The second order correlation represents the statistical properties of quantized light. Heuristically, it can be interpreted as the likelihood of observing a second photon at time $t + \tau$ if the first photon is observed at time t.

The three commonly encountered states of light are as follows:

- **Fock State of Light:**

  It is a special state of light with quantized and well-defined number of photons in it. Often

called *number state*, it is represented by $|n\rangle$. Its $g^{(2)} = \frac{1}{2}$ and the photons like to stay separate from each other in time. This behavior is called anti-bunching [19, 20].

- **Coherent State of Light:**

The coherent state of light is typically produced in laser light. The quantum mechanical wavefunction for the coherent state is represented by

$$|\alpha\rangle = e^{-\frac{|\alpha|^2}{2}} \sum_{n=0}^{\infty} \frac{\alpha^n}{\sqrt{n!}} |n\rangle \qquad Eq.(6.13)$$

where $|n\rangle$ are the number or Fock states and α is a natural number [19, 20].

The coherent light is further holds the following properties:

- It is the eigen state of the photon lowering operator with eigen value α.

$$a|\alpha\rangle = \alpha|\alpha\rangle$$

- $\langle n\rangle = \langle a^{\dagger}a\rangle = |\alpha|^2$

$g^{(2)} = 1$ and the photons are equally spread in time.

- **Thermal State of Light:**

This kind of light is emitted in blackbody radiation of thermal sources. The state is a mixture of different number states with each state's contribution dictated by Maxwell-Boltzmann distribution. Therefore,

$$|\psi_{thermal}\rangle = \sum_{n} P(n)|n\rangle \qquad Eq.(6.14)$$

$$P(n) = e^{-n\frac{\hbar\omega}{\kappa_B T}}\left(1 - e^{-\frac{\hbar\omega}{\kappa_B T}}\right)$$

where T and κ_B are the temperature and Boltzmann constant, respectively. Its $g^{(2)} = 2$ and the photons like to bunch together [19, 20].

Different states of light with 2 photons on average are represented in Fock basis in Figure 13. Furthermore, the $g^{(2)}$ for these three states as initial state of a cavity is shown in Figure 14. For coherent light $g^{(2)} = 1$, which implies that, the photons are equally spaced in time. In chase of thermal light $g^{(2)} = 2$ that indicated that the photons bunch together. However, for Fock light $g^{(2)} = \frac{1}{2}$, an indication of anti-bunching photons that prefer to spread out in time.

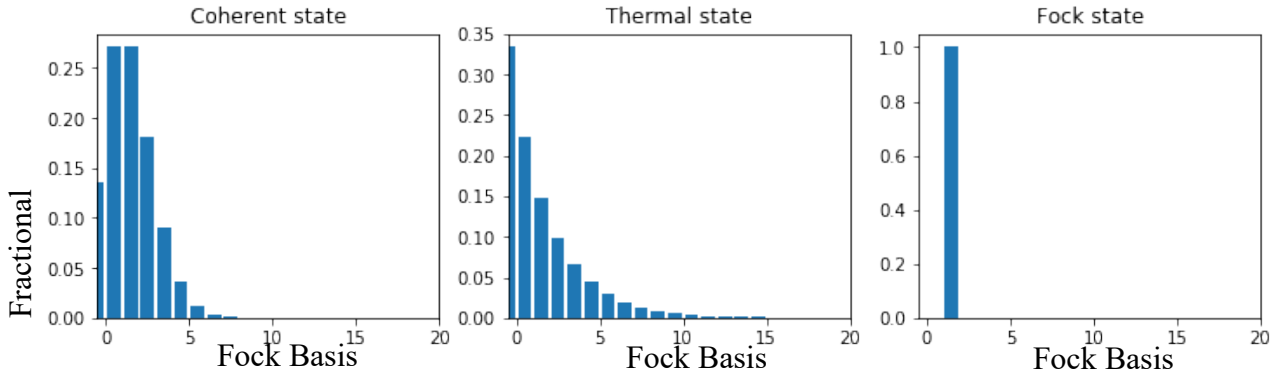

Figure 12: Fock state representation of three states of light with $\langle N_{photon} \rangle = 2$.

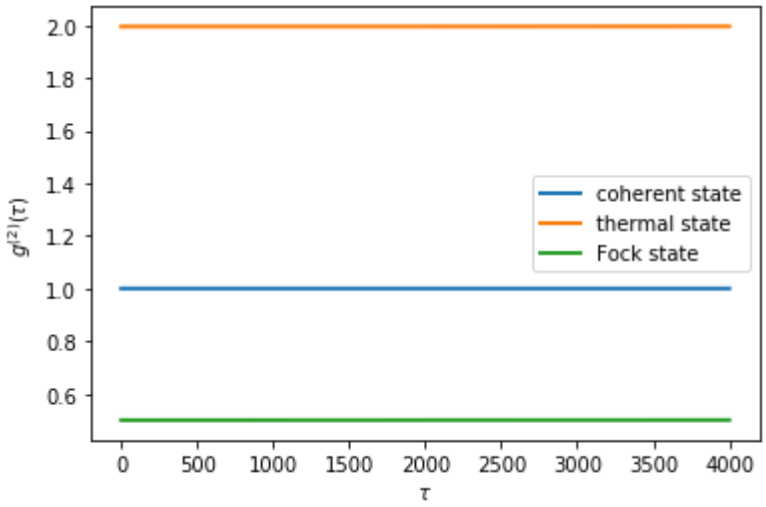

Figure 13: The normalized second order correlation for light leaking from a cavity with initial state as coherent, thermal and Fock states. All have $\langle N_{photon} \rangle = 2$.

The non-normalized version of the second order correlation is shown in the Figure 15. Since the cavity starts with some light that then leaks out without any pumping, the $G^{(2)}$ is a strong indicator of the photon population inside the cavity.

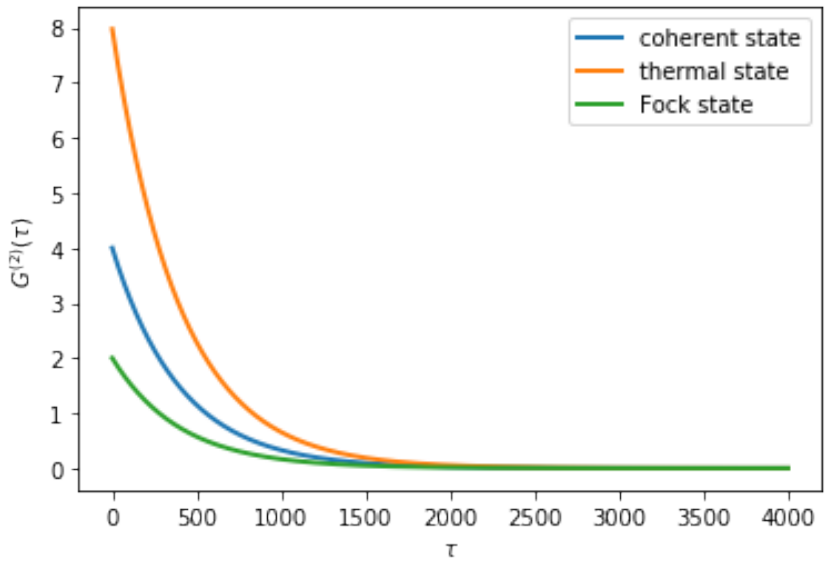

Figure 14: Non-normalized version of the second order correlation for the photons leaking out of the cavity.

However these different states of light have the same output spectrum as evident in Figure 16 and Figure 17. Therefore, while $G^{(1)}$ captures the spectroscopic signature of light-matter interaction, $G^{(2)}$ carries the signature of the nature of light inside the cavity.

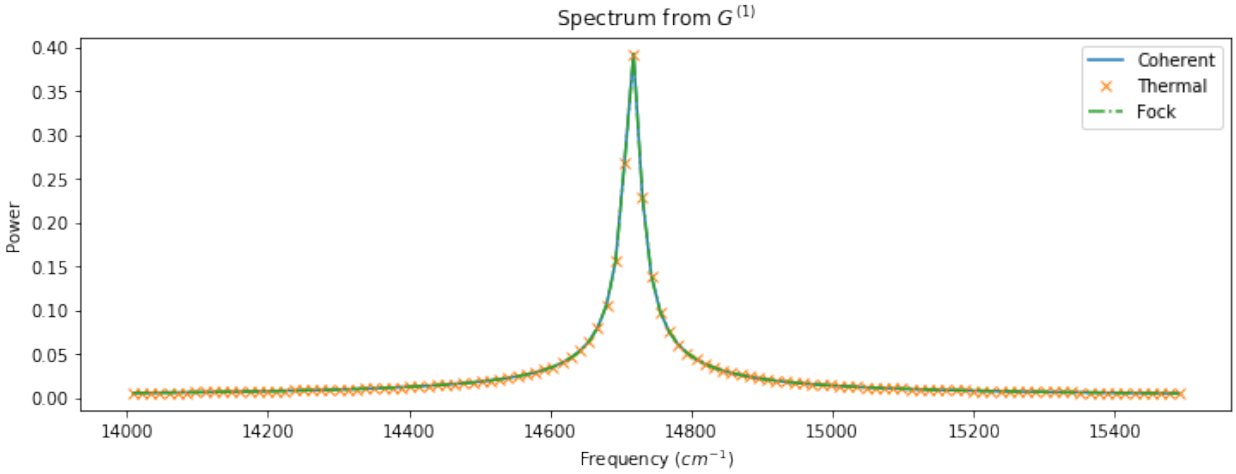

Figure 15: Frequency spectrum from non-normalized first order correlation with different states of light inside cavity.

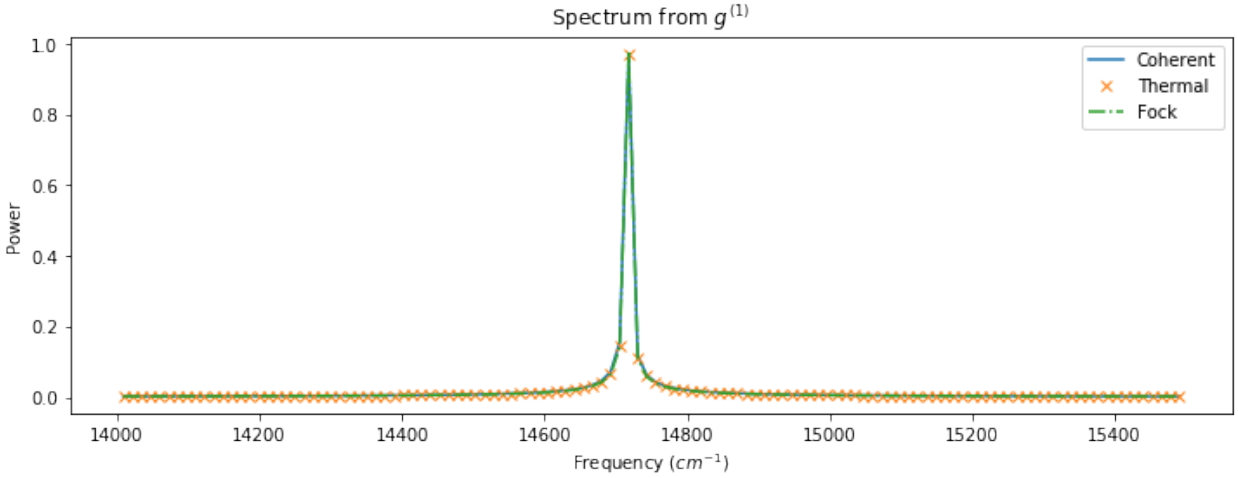

Figure 16: Frequency spectrum from normalized first order correlation with different states of light inside cavity.

CHAPTER 7: LIGHT-MATTER INTERACTION

One Cavity Mode and One Site:

A fully-quantum mechanical interaction between light and matter considers both entities quantized. If a material site with well-defined energy levels is present inside an optical cavity and can interact with the cavity photons, the Hamiltonian can be written as:

$$H_{system} = E_0|0\rangle\langle 0| + \hbar\omega_c a^\dagger a + \hbar\omega_s b^\dagger b + \hbar g(a + a^\dagger)(b + b^\dagger) \qquad Eq.(7.1)$$

where the first terms is the ground state energy for the entire system. It can be removed by a simple energy-shift. a and b are the lowering operators for cavity mode and material site. $\hbar\omega_c$, $\hbar\omega_s$ and $\hbar g$ represent the cavity, site and interaction energies, respectively.

The total system is formally a tensor product of two sub-systems one consisting of the cavity mode and the other consisting of the quantized site. The ladder operators for each sub system and state of the total system is defined as

$$a \equiv a \otimes I_{site}$$

$$b \equiv I_{cavity} \otimes b$$

$$|\psi_{system}\rangle = |n_{cavity}\rangle \otimes |n_{site}\rangle = |n_{cavity}, n_{site}\rangle$$

If the two subsystems are 3-level each, the total possible states will be

$$|n_{cavity}, n_{site}\rangle \in [|0,0\rangle, |0,1\rangle, |0,2\rangle, |1,0\rangle, |1,1\rangle, |2,0\rangle, |2,1\rangle, |1,2\rangle, |2,2\rangle]$$

In general for m subsystems with k levels each, the total number of possible states are k^m. Therefore, in this case, there are 9 possible states. However, if there are only 2 energy quanta in the combined system, the higher energy states are not possible. Because of the energy restriction, the possible states for this total system are

$$|n_{cavity}, n_{site}\rangle \in [|0,0\rangle, |0,1\rangle, |0,2\rangle, |1,0\rangle, |1,1\rangle, |2,0\rangle]$$

And if there is only one quantum of energy total, the possible states further reduce down to

$$\left|n_{cavity}, n_{site}\right\rangle \in [|0,0\rangle, |0,1\rangle, |1,0\rangle]$$

The Hamiltonian of the system can be simplified as

$$H_{system} = \hbar\omega_c a^\dagger a + \hbar\omega_s b^\dagger b + \hbar g(ab + ab^\dagger + a^\dagger b + a^\dagger b^\dagger)$$

$$= \hbar\omega_c a^\dagger a + \hbar\omega_s b^\dagger b + \hbar g(ab^\dagger + a^\dagger b) \qquad Eq.(7.2)$$

where the terms $a^\dagger b^\dagger$ and ab have been thrown out. Since these terms evolve by $e^{i(\omega_c + \omega_s)t}$, removing them is also called the *Rotating Wave Approximation* (RWA). In this form of the Hamiltonian, $ab^\dagger$ removes a photon from the cavity mode and adds an excitation or exciton on matter. Similarly, $a^\dagger b$ creates a photon while simultaneously removing an excitation. Since this energy exchange is scaled by g, it is often called *coupling*. If the size of the material site is much smaller than the wavelength of the cavity mode and electric dipole approximation is applied, the coupling can be related to the radiative lifetime τ through Fermi's golden rule by

$$\frac{1}{\tau} = \frac{2\pi}{\hbar^2}\left|\left\langle n_{cavity}+1, n_{site}-1\middle|\hbar g(ab^\dagger + a^\dagger b)\middle|n_{cavity}, n_{site}\right\rangle\right|^2 \delta(\omega_s - \omega_c)$$

$$= 2\pi g^2\, \delta(\omega_s - \omega_c) \qquad Eq.(7.3)$$

with $n_{cavity} = 0$ and $n_{site} = 1$.

Ignoring the ground state, the Hamiltonian matrix for a system with single quantum of energy is given by

$$H = \begin{bmatrix} \hbar\omega_s & g \\ g & \hbar\omega_c \end{bmatrix} \text{ for } \left|n_{cavity}, n_{site}\right\rangle \in [|0,1\rangle, |1,0\rangle]$$

The corresponding eigenvalues of the Hamiltonian reveal that the new frequencies are moved by the coupling frequency g about the mean of the original frequencies ($\frac{\omega_s+\omega_c}{2}$) that is

$$\frac{1}{2}\hbar\left(\omega_c+\omega_s-\sqrt{(2g)^2+\Delta\omega^2}\right) \text{ and } \frac{1}{2}\hbar\left(\omega_c+\omega_s+\sqrt{(2g)^2+\Delta\omega^2}\right)$$

where $\Delta\omega$ is the difference between the cavity and site frequencies. In a resonant case the about eigenvalues simplify to

$$\frac{\omega_c+\omega_s}{2}-g \text{ and } \frac{\omega_c+\omega_s}{2}+g$$

The cavity frequency can written in terms of the wavevector $\frac{c}{\eta}\sqrt{k_\perp^2+\left(\frac{2}{L}\right)^2}$ for a more general expression. The eigenvectors corresponding to these eigenvalues are

$$|\psi_{lower}\rangle=\frac{1}{\sqrt{2}}|1,0\rangle-\frac{1}{\sqrt{2}}|0,1\rangle$$

$$|\psi_{upper}\rangle=\frac{1}{\sqrt{2}}|1,0\rangle+\frac{1}{\sqrt{2}}|0,1\rangle$$

Each eigenvector is a combination of light and matter wavefunctions. These new combined light-matter states are called *polaritons*. The upper and lower label refers to the frequency of the polaritons as shown in Figure 17. At $k_\perp=0$, the separation between the upper and lower polariton frequencies is $2g$. This is further explored in Figure 18, which shows the frequencies for different values of coupling. As the coupling increases, the difference between the eigen-frequencies increases.

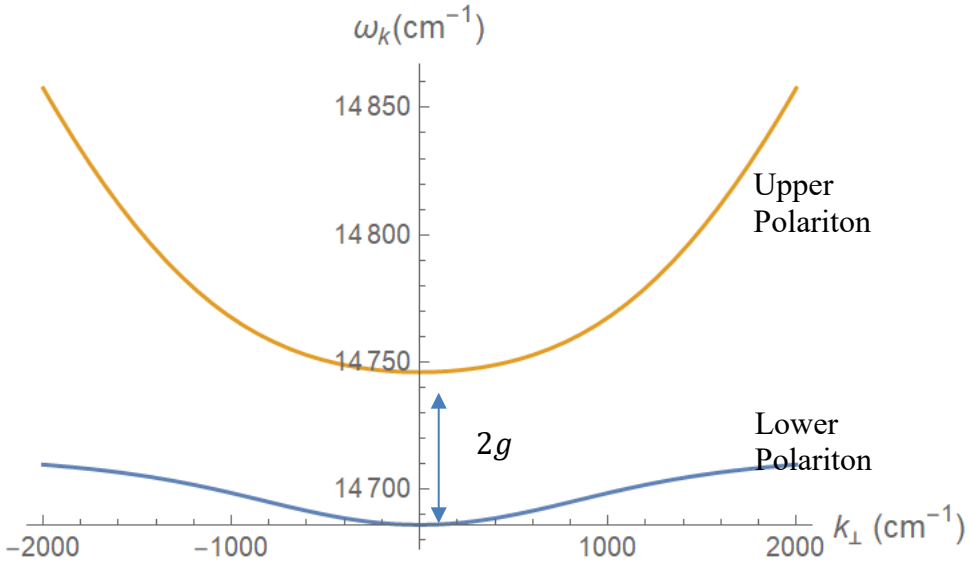

Figure 17: The dispersion relation for upper and lower polaritons for g=30 cm^{-1}.

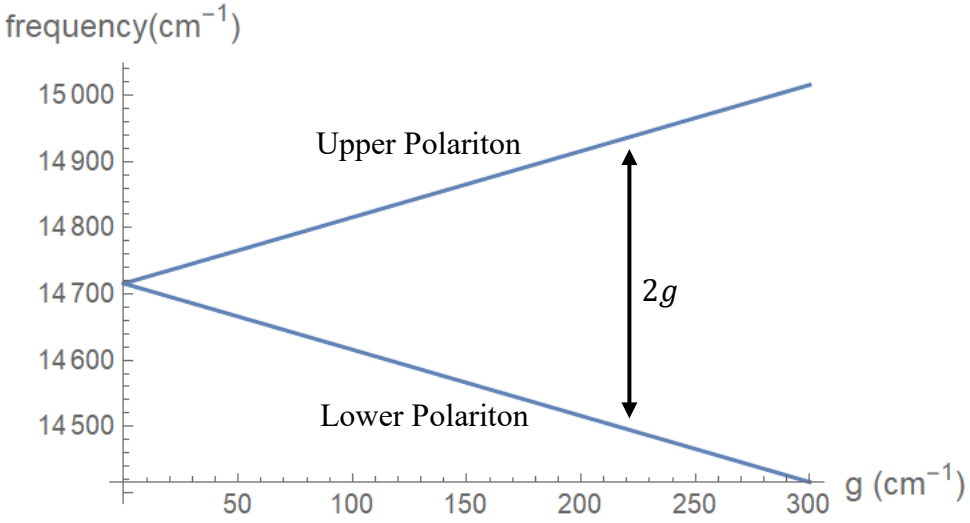

Figure 18: Frequencies for the eigen-energies. The frequencies are shown as a function of the coupling g for the cavity-site system on resonance at 14716 cm^{-1} with $k_\perp = 0$.

However, if the total system is allowed up to 2 photons, the Hamiltonian and states are given by

$$H = \begin{bmatrix} \hbar\omega_s & g & 0 & 0 & 0 \\ g & \hbar\omega_c & 0 & 0 & 0 \\ 0 & 0 & 2\hbar\omega_s & \sqrt{2}g & 0 \\ 0 & 0 & \sqrt{2}g & \hbar\omega_s + \hbar\omega_c & \sqrt{2}g \\ 0 & 0 & 0 & \sqrt{2}g & 2\hbar\omega_c \end{bmatrix} \text{ for } |n_{cavity}, n_{site}\rangle$$

$$\in [|0,1\rangle, |1,0\rangle, |0,2\rangle, |1,1\rangle, |2,0\rangle]$$

The eigenvalues of this new Hamiltonian are

$$\hbar(\omega_c + \omega_s), \hbar\left(\omega_c + \omega_s + \sqrt{(2g)^2 + \Delta\omega^2}\right), \hbar\left(\omega_c + \omega_s - \sqrt{(2g)^2 + \Delta\omega^2}\right), \frac{\hbar}{2}\left(\omega_c + \omega_s + \sqrt{(2g)^2 + \Delta\omega^2}\right), \frac{\hbar}{2}\left(\omega_c + \omega_s - \sqrt{(2g)^2 + \Delta\omega^2}\right)$$

In addition to the two previous frequencies distributed around the $\frac{\omega_s+\omega_c}{2}$, the new eigenvalues contain 3 more frequencies called over-tones that are at and around $\omega_s + \omega_c$. The states corresponding the new frequencies are a linear combination of the states with 2 unites of energy such that

$|P_i\rangle = \alpha_i|2,0\rangle + \beta_i|1,1\rangle + \gamma_i|0,2\rangle$ for some numbers α_i, β_i and γ_i. The energy level diagram for these 1 and 2 photon eigenvalues is shown in Figure 20 for $k_\perp = 0$. A full dispersion relation for the three higher energy eigenvalues is shown in Figure 21.

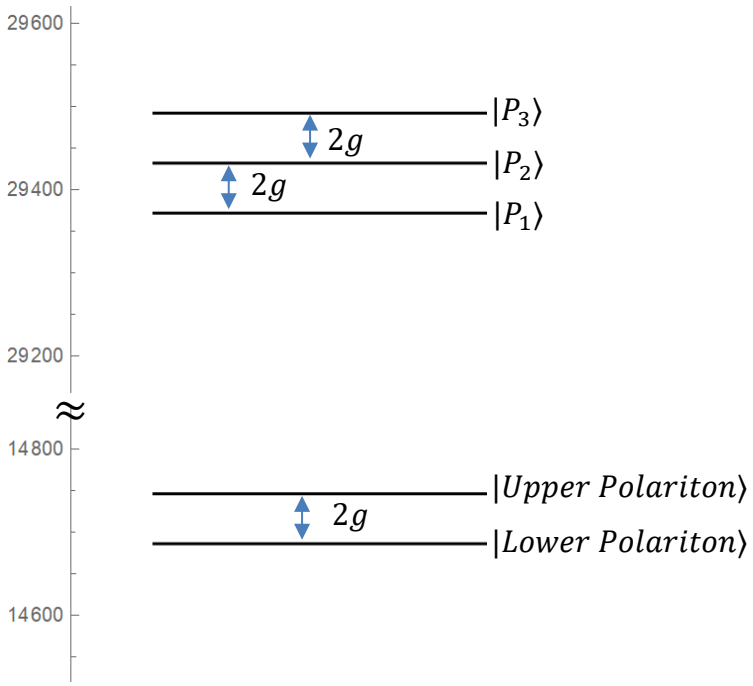

Figure 19: One site and one cavity mode system on resonance with g=30 cm^{-1},ω_c=ω_s=14716.33 cm^{-1}. With 2 energy units in total, there are 2 sets eigen energies. One is centered on the cavity frequency and the other is centered at twice the cavity frequency. This second set is termed overtones.

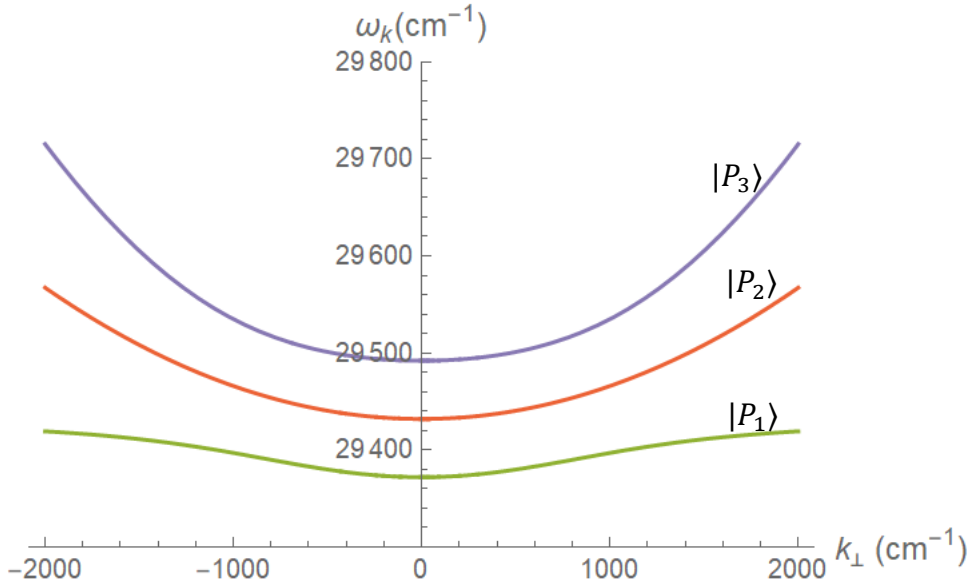

Figure 20: The dispersion relation for the upper three energy levels for a cavity-site system with 2 units of energy.

If the cavity is on resonance with the site, the Hamiltonian matrix simplifies to

$$H = \begin{bmatrix} \hbar\omega & g & 0 & 0 & 0 \\ g & \hbar\omega & 0 & 0 & 0 \\ 0 & 0 & 2\hbar\omega & \sqrt{2}g & 0 \\ 0 & 0 & \sqrt{2}g & 2\hbar\omega & \sqrt{2}g \\ 0 & 0 & 0 & \sqrt{2}g & 2\hbar\omega \end{bmatrix}$$

with eigen-frequencies $\omega - g, \omega + g, 2(\omega - g), 2\omega$ and $2(\omega + g)$. The corresponding eigenvectors are

$$|\psi_{lower}\rangle = \frac{1}{\sqrt{2}}|1,0\rangle - \frac{1}{\sqrt{2}}|0,1\rangle$$

$$|\psi_{upper}\rangle = \frac{1}{\sqrt{2}}|1,0\rangle + \frac{1}{\sqrt{2}}|0,1\rangle$$

$$|P_1\rangle = \frac{1}{2}|2,0\rangle - \frac{1}{\sqrt{2}}|1,1\rangle + \frac{1}{2}|0,2\rangle$$

$$|P_2\rangle = \frac{1}{\sqrt{2}}|2,0\rangle - \frac{1}{\sqrt{2}}|0,2\rangle$$

$$|P_3\rangle = \frac{1}{2}|2,0\rangle + \frac{1}{\sqrt{2}}|1,1\rangle + \frac{1}{2}|0,2\rangle$$

In an ideal cavity with energy conservation, the three high-energy polaritons do not transition to the two lower energy polaritons because the higher energy ones are linear combination of the Fock states with two energy units and the lower energy ones are made of Fock states with one energy unit. However, in a leaky cavity, the energy conservation does not apply and the photons can leak out. The collapse operator that corresponds to the cavity leakage can take a system prepared in any of the three high-energy polaritons to the two low-energy polariton and then to the vacuum state.

Using the site-cavity Hamiltonian in the Master Equation formalism described earlier, the time evolution of the total system state can be computed for a leaky cavity (as described

previously). The programming is done in Python and the code is provided in the appendix. The main library used in the programing is Qutip [22, 23]. Qutip is a library specifically programmed to handle fully quantum interactions for a given system with master equation. The starting state of the system is a two-photon Fock state with no excitation on the site. The time dependent population of the site-cavity system at resonance on $14716.33\ cm^{-1}$ is shown in Figure 22. These results indicate that the overall energy is lost through cavity leakage but during this time, the populations of the site and the cavity oscillate in a process called Rabbi Oscillation. As the coupling increases, the oscillation frequency increases.

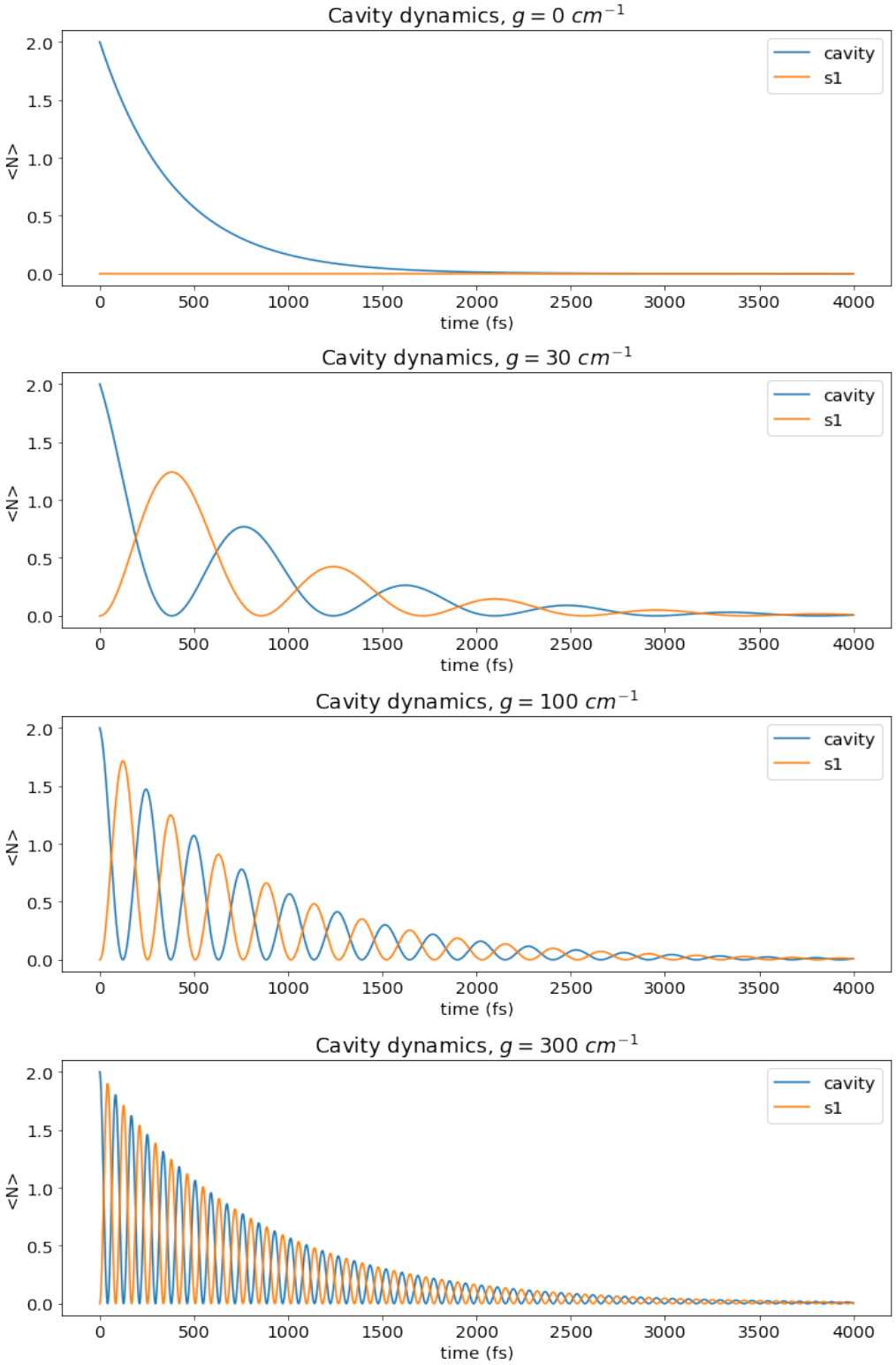

Figure 21: Cavity-site system with leaky cavity on resonance with site at 14716 cm^{-1}. Each plot shows the evolution of the population for the cavity mode and the site as a function of time for different values of the coupling g.

The first order coherence and its Fourier transform for the photons leaking out of the cavity is showing in Figure 23 and Figure 24. The energy and hence the frequency for these results have been shifted to have zero at $14716\ cm^{-1}$. There are two peaks apparent in the frequency spectrum, an indication of the two fundamental modes. As the cavity-site coupling increases, the split between the frequencies grows.

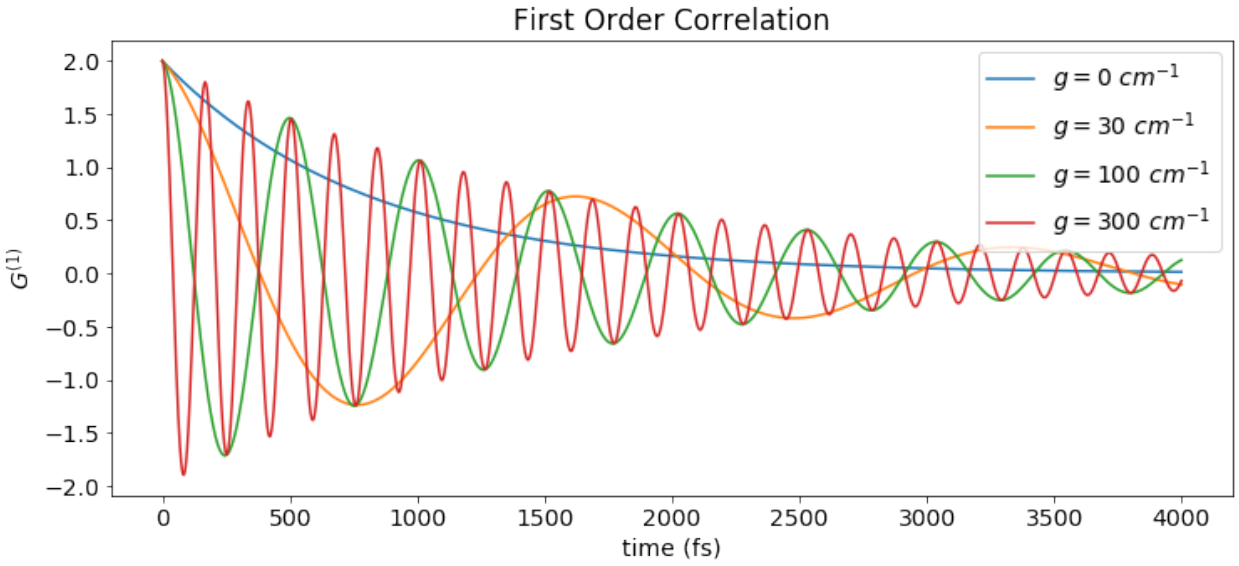

Figure 22: First order correlation for a frequency shifted cavity-site system starting of with 2 photons in the cavity mode. The mirror transmission for the cavity is 0.25 %. *As the coupling increases the oscillations increase as well.*

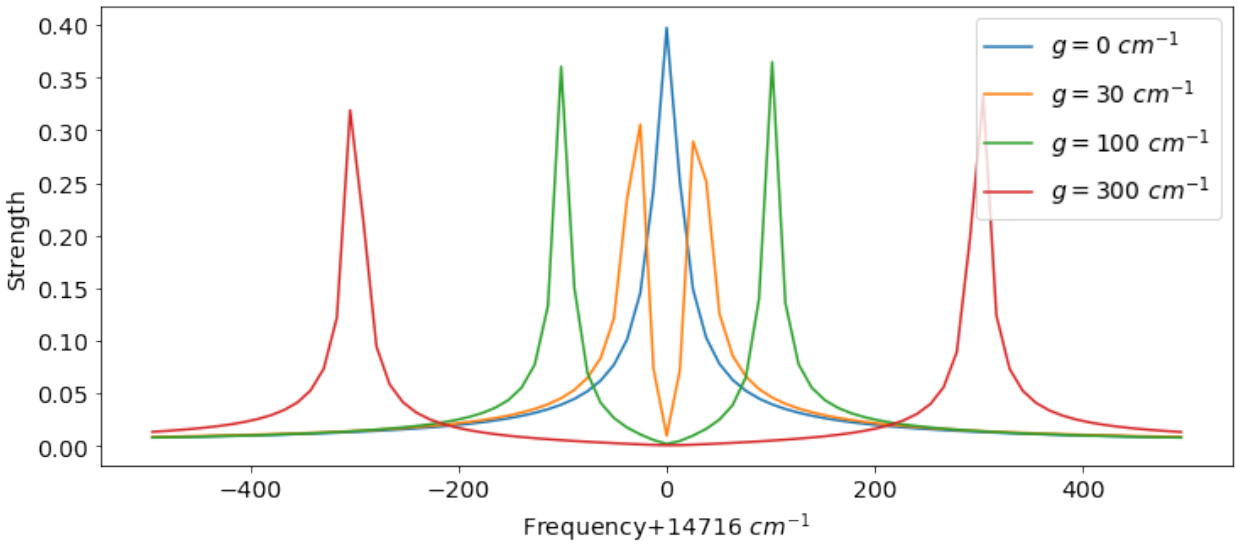

Figure 23: Frequency spectra associated with single site-cavity model starting in a 2 photon Fock state. The spectra are for different values of coupling showing the fundamental modes of the total system.

The second order correlation for the output photons is shown in Figure 25. However, it's normalized version is not useful as it contains divergences due to the cavity's photon population oscillating to zero. In the absence of any source to maintain a steady population of photons in the cavity, only the non-normalized version of the second order correlation makes physical sense. These plots indicate that the cavity photons shows a Fock-state nature.

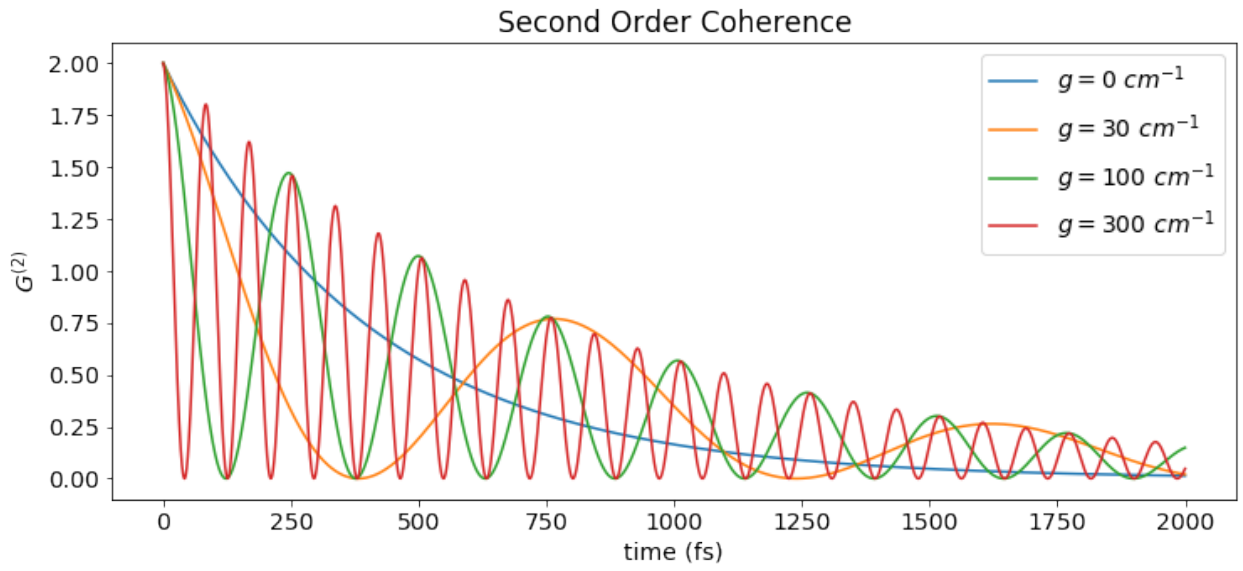

Figure 24: Second order correlation for the photons leaking out of the cavity for different light-matter couplings.

The site has been considered a perfect harmonic oscillator so far. However, the harmonic potential is only an approximation to an otherwise complex potential profile in most material systems. The deviation from the true potential is negligible for ground and first excited state but for higher excited states, it becomes significant. This modifies the site energies away from those of the harmonic oscillator. Furthermore, in systems with multiple sites, there can be many options to distribute the energy. In such systems, the overall energy will be higher if all the excitations are focused on a single site. These artifacts can be captured in a new term defined as the *anharmonicity*. The modified Hamiltonian is given by.

$$H_{system} = \hbar\omega_c a^\dagger a + \hbar\omega_s b^\dagger b + \hbar g(ab^\dagger + a^\dagger b) + \hbar u b^\dagger b^\dagger bb$$

Here u is a positive number and for a site with n excitations, the last terms adds $u \times n(n+1)$ energy to the system. Consequently, the overtones in the eigenvalues of the Hamiltonian are affected by this energy cost as shown in Figure 26. With the anharmonicity factor in the Hamiltonian, the time evolution of the system leads to following population dynamics (Figure

27). The results indicate an additional modulation on top of the cavity decay and Rabi Oscillations. The new modulation is more pronounced in high coupling.

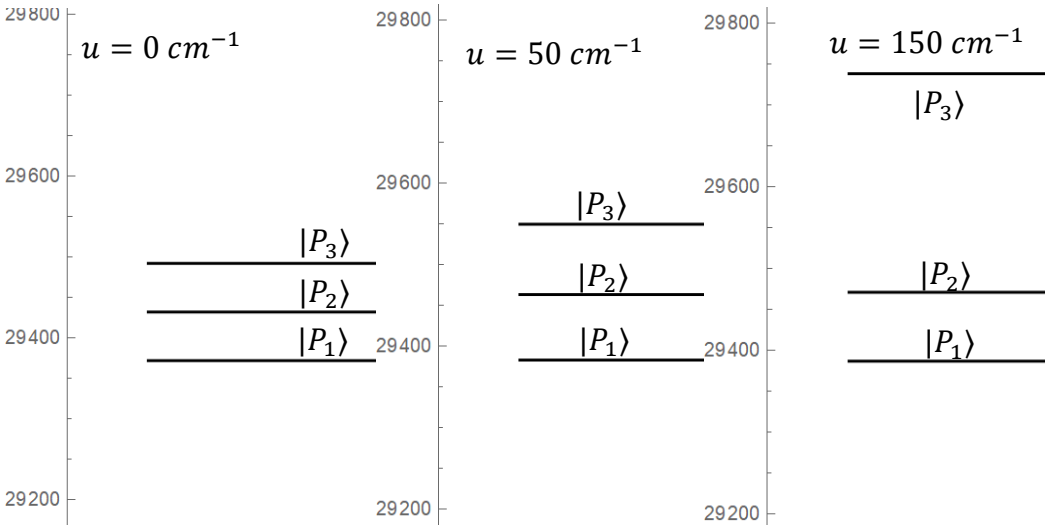

Figure 25: Overtones are shown for one cavity-one site system with 2 photons. The anharmonicity increases the energy for high energy level even higher. The cavity is on resonance with site at ω_c=14716 cm^{-1} and $g = 30\ cm^{-1}$.

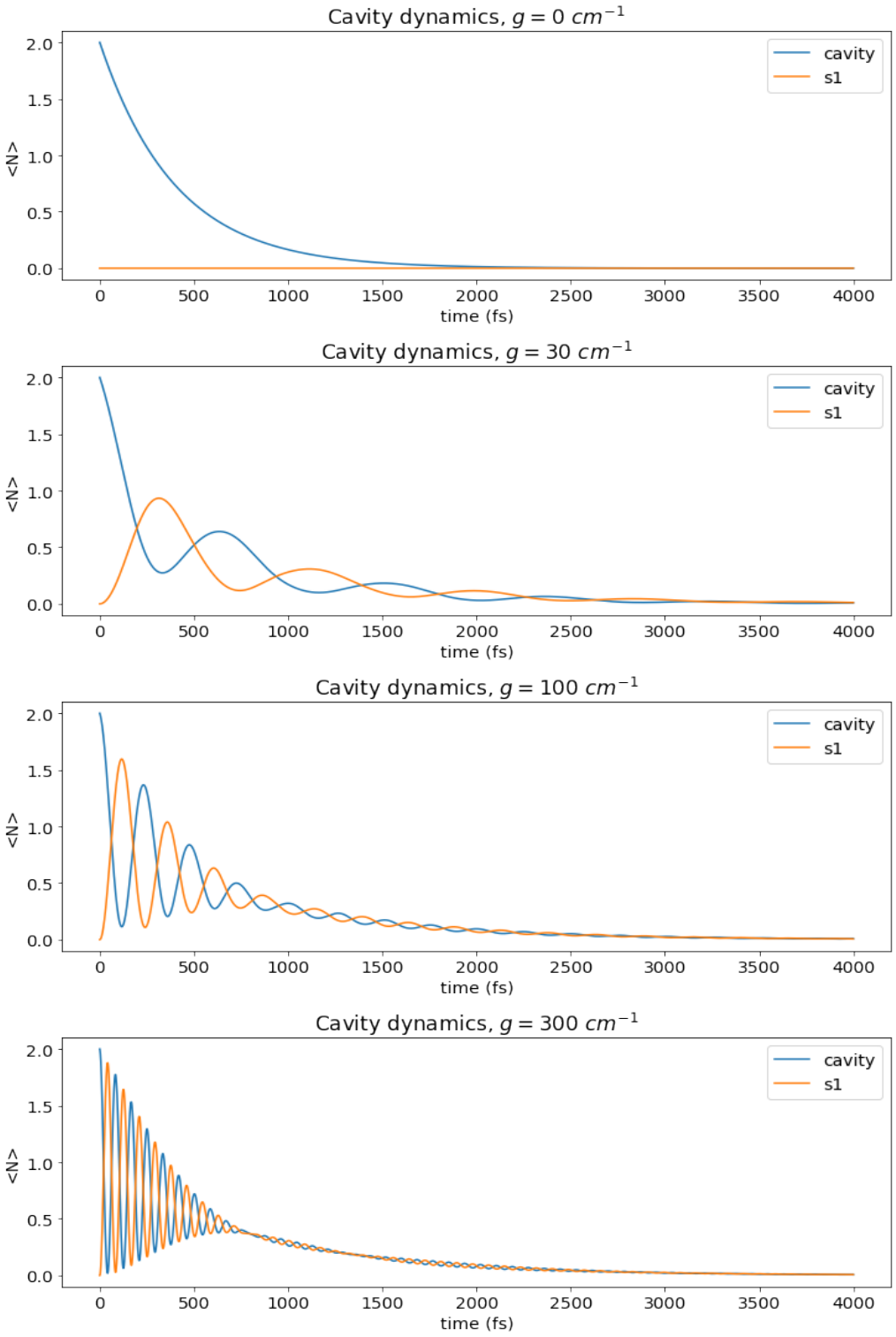

Figure 26: The evolution of excitation and photon population with anharmonicity of $u = 50\ cm^{-1}$.

The anharmonicity also affects the $G^{(1)}$ and spectrum of the photons leaking out of the cavity. The spectrum is shown in Figure 28. It indicates additional splitting and suppression of higher frequency strengths.

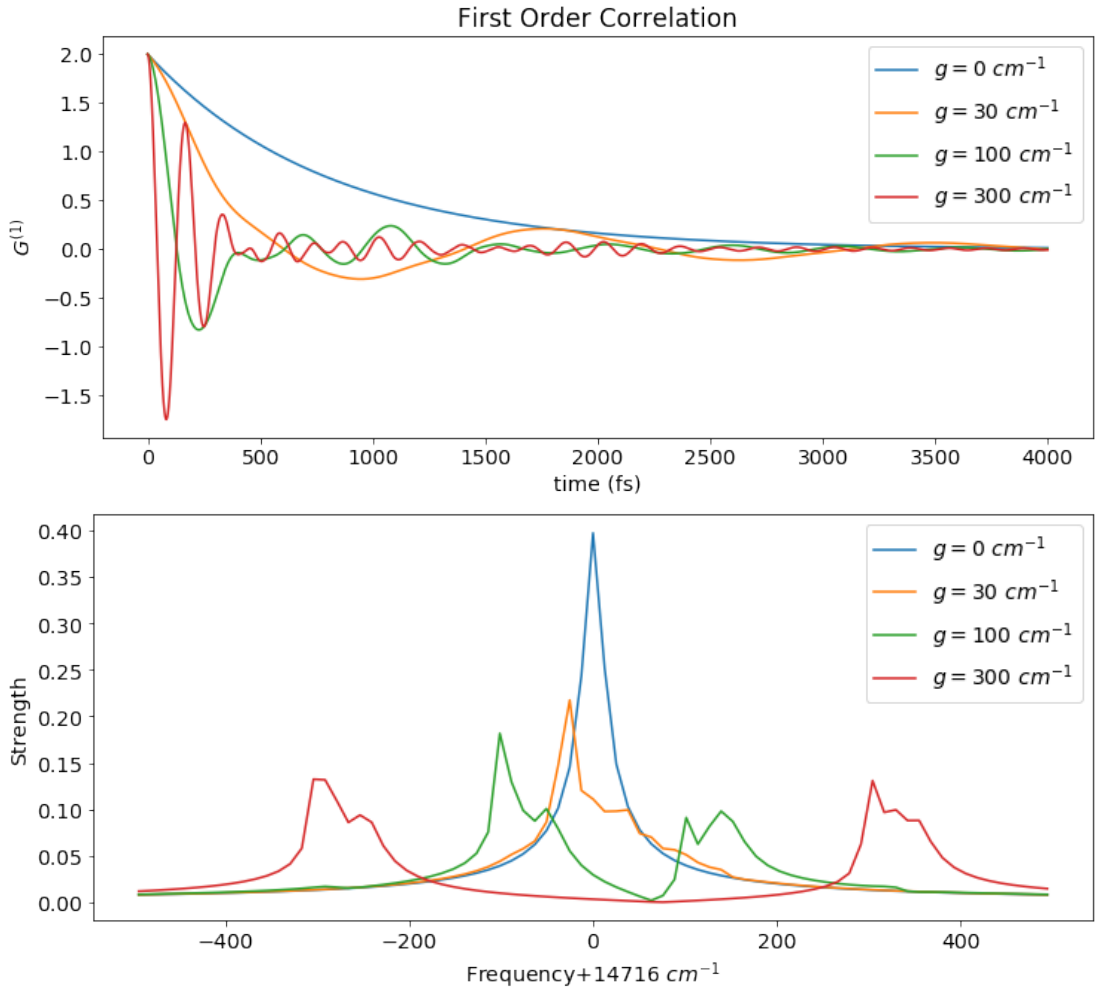

Figure 27: Effects of the anharmonicity on the first order correlation and frequency spectrum for different coupling strengths.

However, the second order correlation does not show any significant change with the addition of anharmonicity as shown in Figure 29.

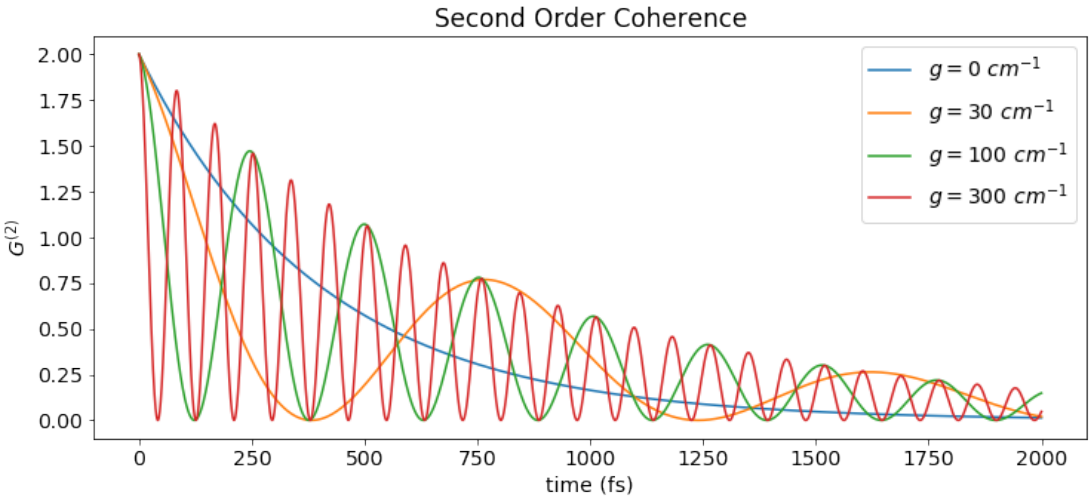

Figure 28: Second order correlation for system with anharmonicity.

Since the weak-field limit and rotating wave approximation is used in this mode, for the upcoming systems the coupling of $g = 30\ cm^{-1}$ will be used. Furthermore, the anharmonicity will either be zero or $u = 50\ cm^{-1}$.

CHAPTER 8: ONE CAVITY MODE AND TWO SITES

With only one site in the cavity, the types of interactions are limited. However, consider a system consisting of two sites and one cavity mode. This corresponds to a system with chromophores that can interact with the cavity mode and exchange excitation with each other. The sites can now exchange energy with the cavity mode and with each other. The generalized Hamiltonian is given by

$$H_{system} = \hbar\omega_c a^\dagger a + \sum_s \hbar\omega_s b_s^\dagger b_s + \sum_s \hbar g\left(a b_s^\dagger + a^\dagger b_s\right) + \hbar t\left(b_1 b_2^\dagger + b_1^\dagger b_2\right) + \sum_s \hbar u b_s^\dagger b_s^\dagger b_s b_s \qquad Eq.(8.1)$$

The first two terms encode the energy contained in the cavity mode and on the two sites, respectively. The third term represents the light-matter interaction. In the third term, t represents the hopping of excitation from one site to another as $b_1 b_2^\dagger$ removes an excitation from site 1 and adds it to site 2 ($b_1^\dagger b_2$ does the reverse). Finally, the fifth term represents the anharmonicity (u) which is the energy cost associated with placing multiple excitations on the same site. Possible states and the Hamiltonian for a total of 2 energy units is shown in Table 1. The notation for states follows $|n_{cavity}, n_{site1}, n_{site2}\rangle$. For clarity, only non-zero terms are not shown.

Table 1: The Hamiltonian for two sites and a cavity mode in number basis. Only non-zero values are shown for clarity

	$\|0,1,0\rangle$	$\|0,0,1\rangle$	$\|1,0,0\rangle$	$\|0,2,0\rangle$	$\|0,1,1\rangle$	$\|0,0,2\rangle$	$\|1,1,0\rangle$	$\|1,0,1\rangle$	$\|2,0,0\rangle$
$\|0,1,0\rangle$	ω_1	t	g						
$\|0,0,1\rangle$	t	ω_2	g						
$\|1,0,0\rangle$	g	g	ω_c						

$\|0,2,0\rangle$				$2\omega_1 + 2u$	$\sqrt{2}t$		$\sqrt{2}g$		
$\|0,1,1\rangle$				$\sqrt{2}t$	$\omega_1 + \omega_2$	$\sqrt{2}t$	g	g	
$\|0,0,2\rangle$					$\sqrt{2}t$	$2\omega_2 + 2u$		$\sqrt{2}g$	
$\|1,1,0\rangle$				$\sqrt{2}g$	g		$\omega_c + \omega_1$	t	$\sqrt{2}g$
$\|1,0,1\rangle$					g	$\sqrt{2}g$	t	$\omega_c + \omega_2$	$\sqrt{2}g$
$\|2,0,0\rangle$							$\sqrt{2}g$	$\sqrt{2}g$	$2\omega_c$

The analytical expressions for the eigen-values of this system are complicated; however, the energy level diagrams shows the fundamental frequencies have 3 modes and the overtones contain 6 modes. In the spirit of the example continued so far, the energy level diagram shown in Figure 30 corresponds to a system with $g = 30\ cm^{-1}, t = 0\ cm^{-1}$ and $u = 0\ cm^{-1}$. The site frequencies are $\omega_{s1} = 14716\ cm^{-1}$ and $\omega_{s2} = 14787\ cm^{-1}$. The cavity frequency is at the center of the two site frequencies at $\omega_c = 14763\ cm^{-1}$. Consequently, the fundamental modes are around the cavity frequency and the overtones are around twice the cavity frequency.

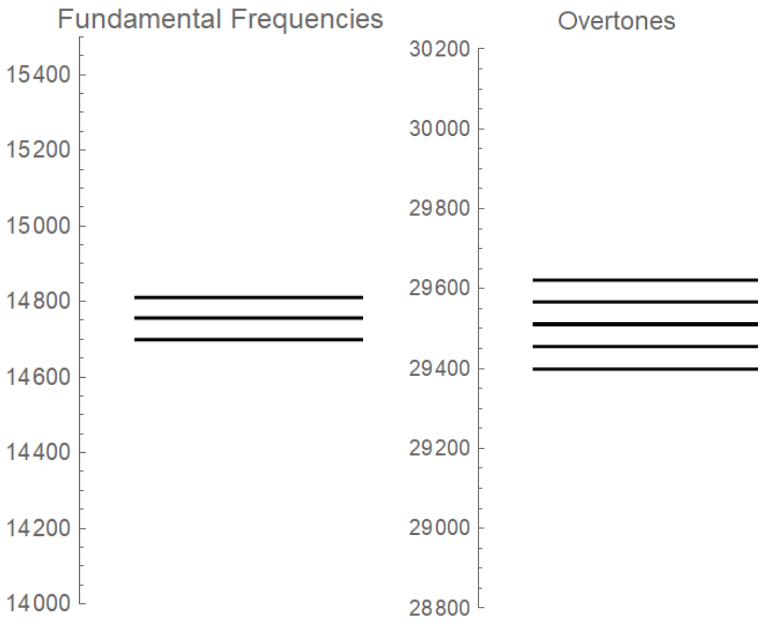

Figure 29: Fundamental frequencies and overtones for the 2 sites in a cavity. The light-matter coupling is $g = 30\ cm^{-1}$.

Effect of Hopping:

Since two sites are present in the cavity, a non-zero hopping term allows the excitations to transfer from one site to another. Phenomenologically, hopping is the energy transfer through dipole-dipole interaction of the two sites. This new channel of energy transfer not only changes the population dynamics inside the cavity, but also affects the spectrum and second order correlations of the photons leaking out of the cavity. Experimentally, t can be determined though time resolved spectroscopy that can probe the absorption on one site and emission from other. If the value of t is positive, the hopping adds an extra energy to the overall Hamiltonian. On the other hand, a negative valued t decreases the overall energy. Practically, these two scenarios are often observed in H and J aggregates of fluorescent molecules, respectively. The presence of hopping affects both fundamental modes and the overtones as evident in Figure 31.

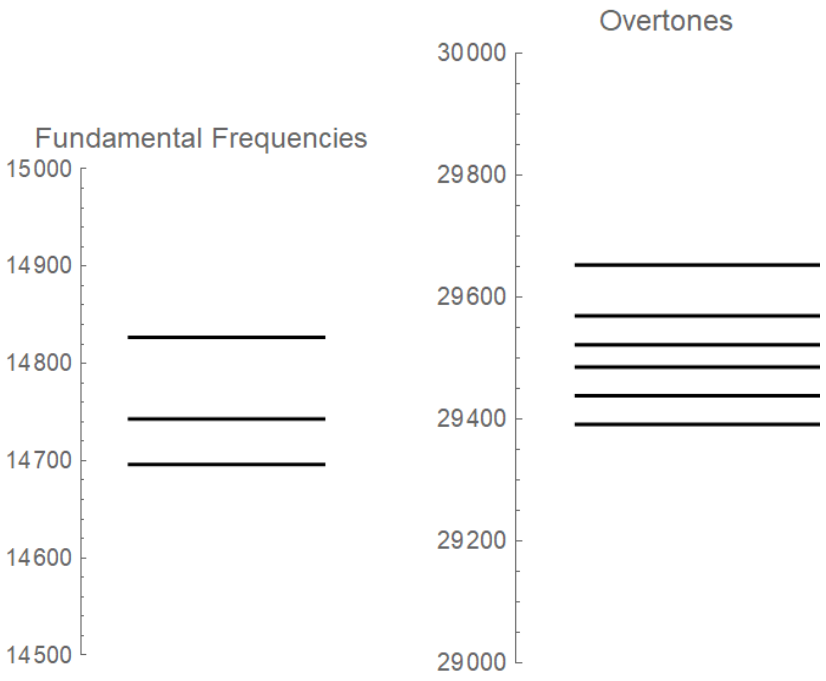

Figure 30: Energy level diagram for the eigenvalues of the 2 site-one cavity system with g=30 cm^{-1}, u=0 cm^{-1}, and $t = 36\ cm^{-1}$. The presence of hopping energy shifts both the fundamental modes and the overtone.

In Figure 32, the evolution of population in the cavity mode and the sites is shown as a function of the site-site hopping. When hopping is zero, the population of both sites behave identically. However, in the presence of non-zero hopping one site gains excitations more readily then the other. The higher energy site (site 2) gains more excitations in the presence of positive hopping and the lower energy site (site 1), in the negative hopping. However, as the strength of hopping increases, the sites exchange energy more readily and their populations follow each other more closely.

The positive and negative values of hopping affect the first order correlation and spectra of the leaking photons uniquely. As shown in Figure 33, the positive values downshift and the negative values upshift the frequency along with an inhomogeneous broadening effect.

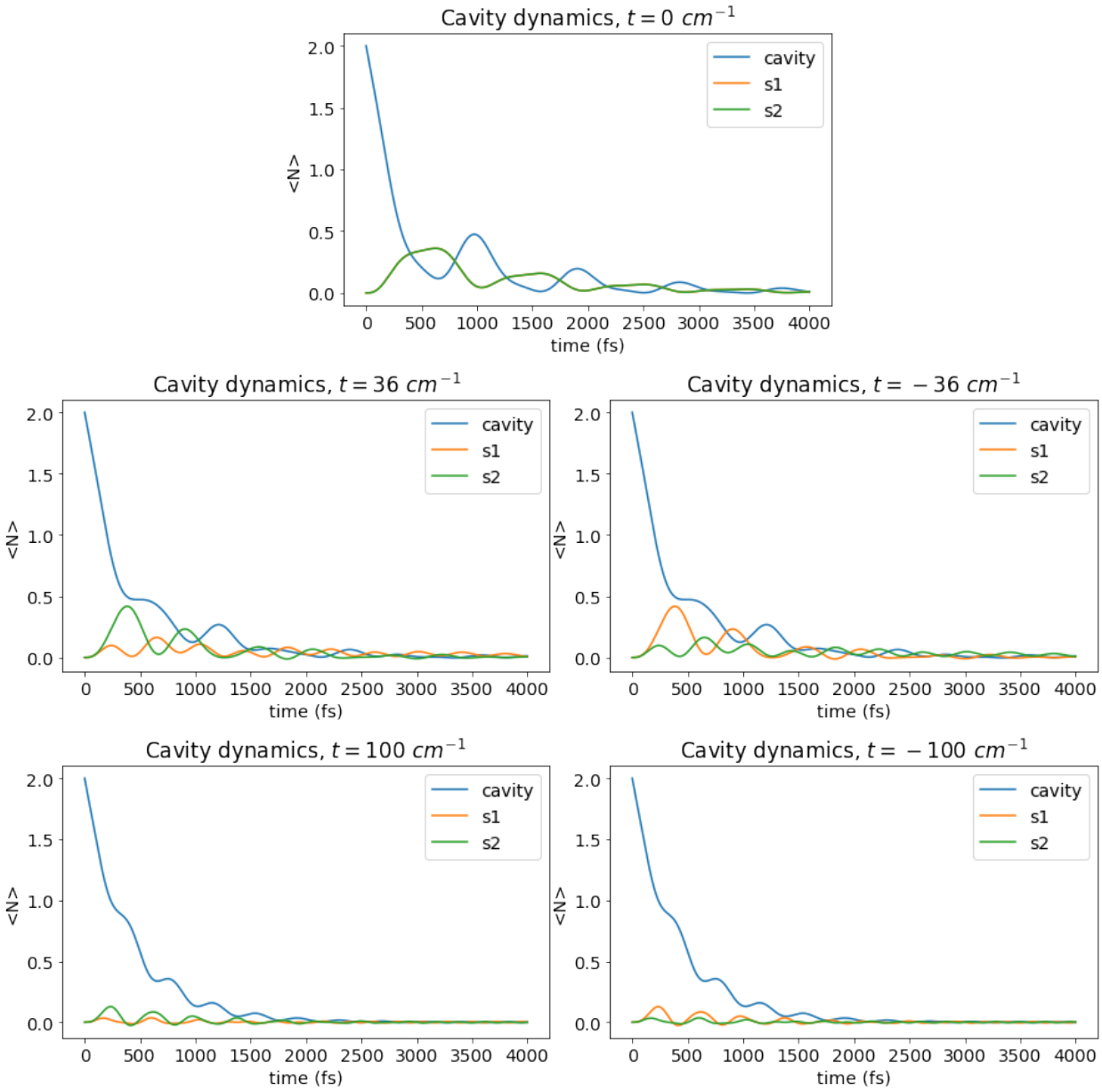

Figure 31: Population dynamics inside the cavity for different values of t with $g = 30\ cm^{-1}$ and $u = 0\ cm^{-1}$. The cavity frequency is $\omega_c = (\omega_{s1}+\omega_{s2})/2$ and $\omega_{s1}<\omega_{s2}$.

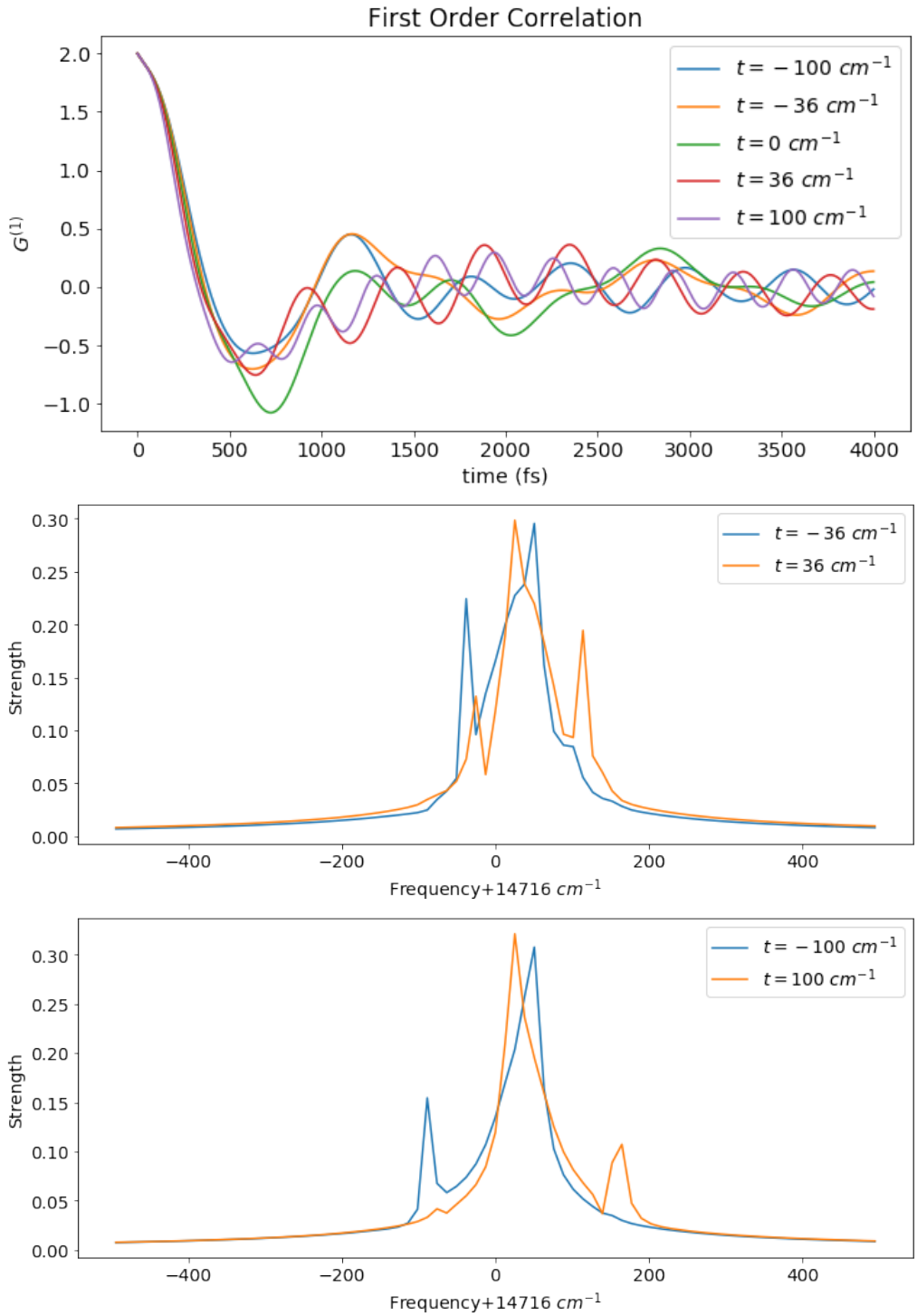

Figure 32: First order correlation and spectra for different values of hopping. For this system g=30 cm^{-1} and u=0 cm^{-1}.

The dynamics of the photon population inside the cavity and the second order correlation in the output photons, both depend only on the magnitude of hopping. The positive or negative sign of the hopping has not effect these properties. These results are shown in Figure 34.

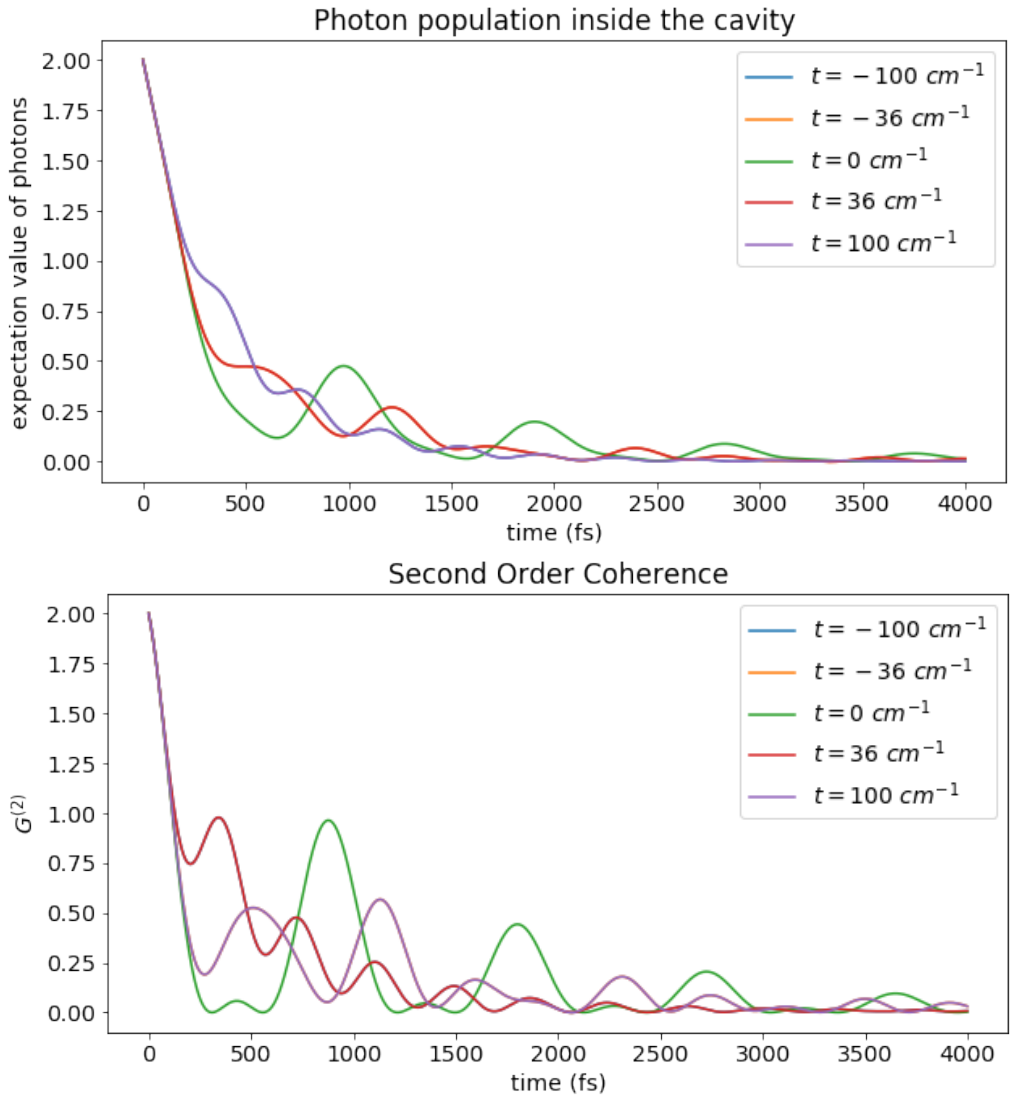

Figure 33: Photon population in the cavity (top) and second order correlation (bottom) for different values of hopping. For this system g=30 cm^{-1} and u=0 cm^{-1}

Effect of Anharmonicity:

The presence of anharmonicity in the system raises the energy of the states with more than one excitation on any site. Consequently, only the high-energy (overtones) eigenvalues of the Hamiltonian are affected. However, the population dynamics inside the cavity, first and second order correlations, and spectrum of the output photons are unaffected.

The presence of anharmonicity does affect the spectrum and correlations if the cavity frequency is on resonance with any of the site. The effects of resonance of the cavity mode and site frequencies are explored in the next section.

Effect of Resonance:

The effects of hopping and anharmonicity have been explored in the previous sections for a system where cavity frequency is in the center of the site one and site two frequencies. However, if the cavity frequency is on resonance with anyone of the sites, that site is more able to increase excitation population more readily than the other. To test the new dynamics introduced by the resonance, the time evolution of system is computed with $g = 30\ cm^{-1}$, $u = 50\ cm^{-1}$ and $\omega_c = \omega_{s1}$ or ω_{s2}.

With cavity on resonance with site 1, the population dynamics is displayed in Figure 35 for different values of t. It is evident that even in the absence of hopping ($t = 0\ cm^{-1}$), the population of site 1 increases and behaves differently than that of site 2.

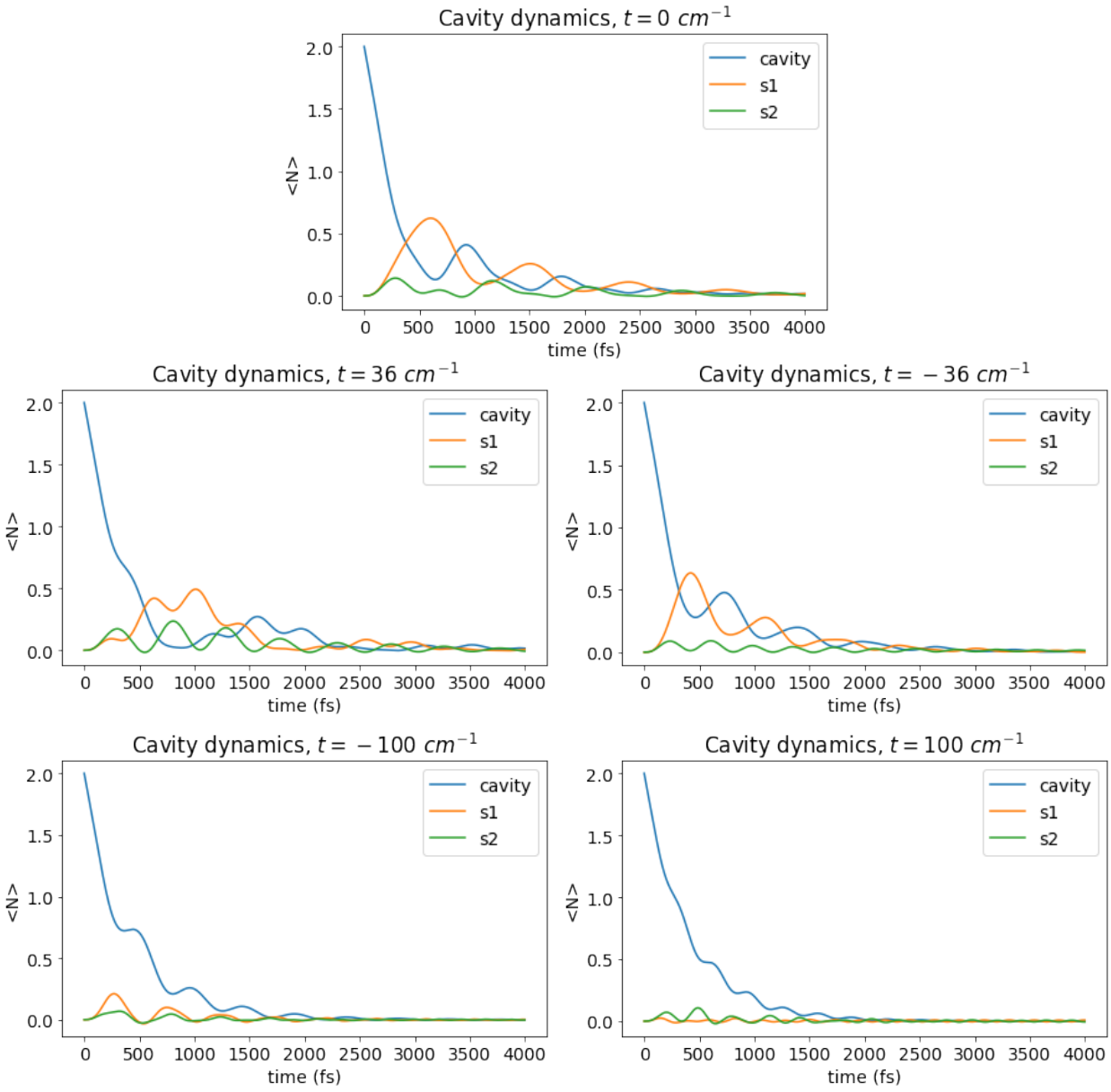

Figure 34: Population dynamics inside the cavity for different values of t with g=30 cm^{-1} and u=50 cm^{-1}. The cavity frequency is $\omega_c = \omega_{s1}$ and $\omega_{s1}<\omega_{s2}$.

With $t = 36\ cm^{-1}$, previously the site 2 population increased more rapidly than site 1; however, with the cavity frequency on resonance with site 1, its population peaks higher than site 2.

Similarly, the frequency spectrum of the output photons and the second order correlation change. These changes are shown in Figure 36 and Figure 37 respectively.

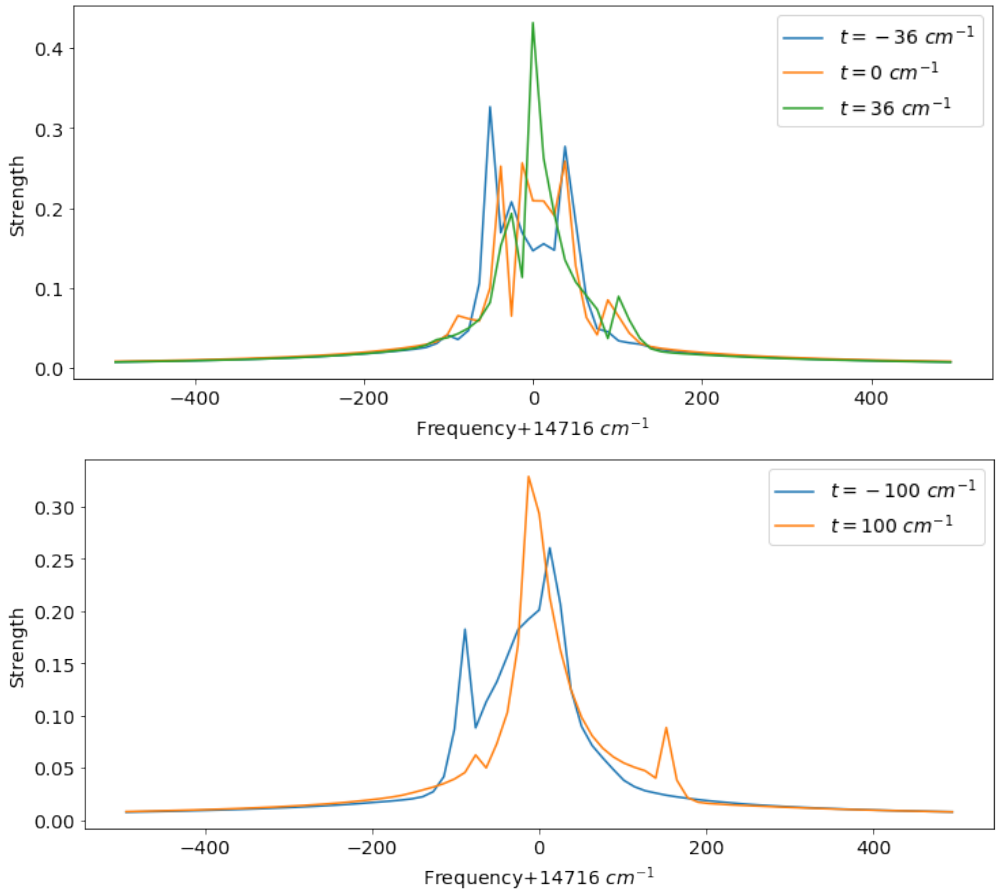

Figure 35: Frequency spectrum from first order correlation of photons leaking from cavity. The cavity is on resonance with the frequency of site 1. The coupling and anharmonicity are g=30 cm^{-1} and u=50 cm^{-1}.

When cavity frequency was in between the site 1 and site 2 frequencies, the second order correlation did not show any difference with the change in the sign of hopping. However, with the cavity resonant with site 1, the every value of hopping has a unique signature on the photon statistics (Figure 37).

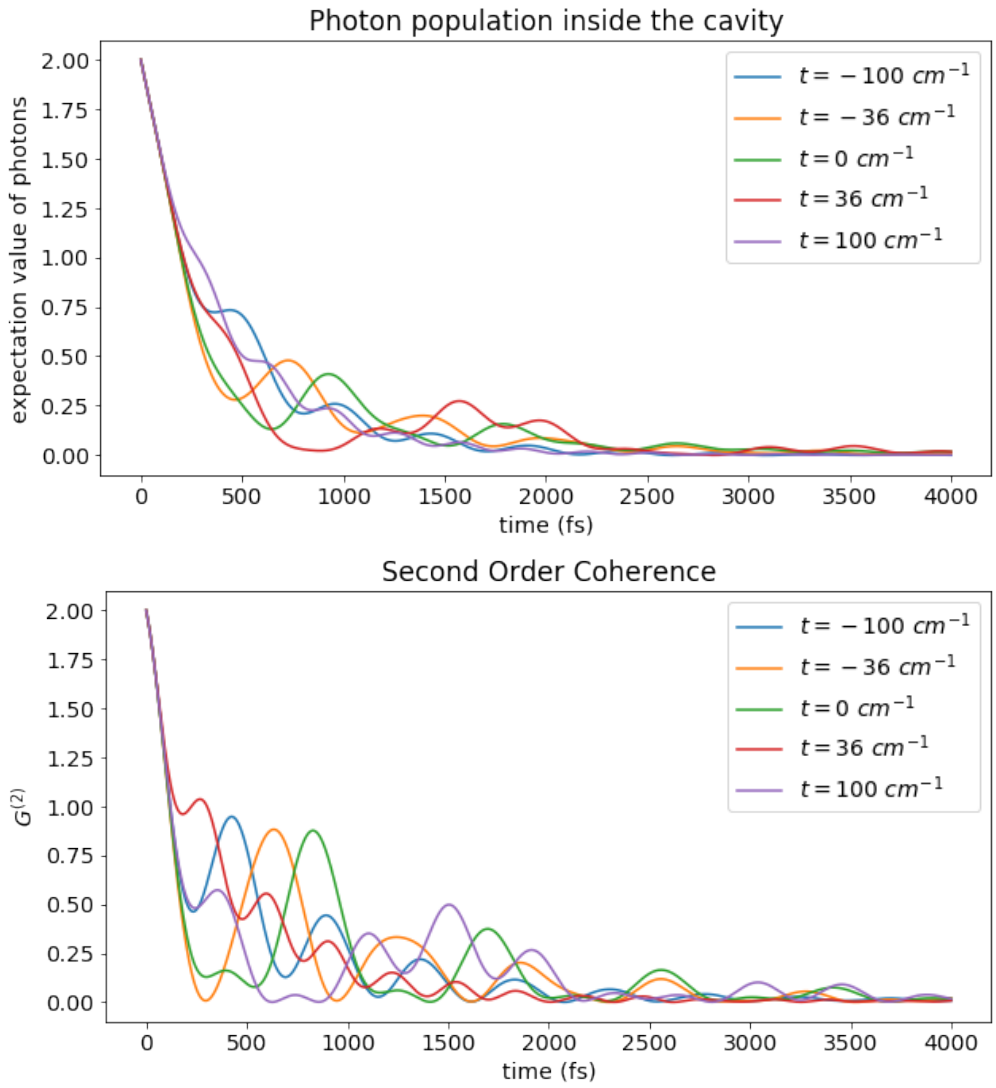

Figure 36: Photon population inside the cavity and second order coherence for photons leaking from cavity. The cavity is on resonance with the frequency of site 1. The coupling and anharmonicity are g=30 cm^{-1} and u=50 cm^{-1}.

CHAPTER 9: LIGHT HARVESTING COMPLEX II

LHCII is one of the most abundant light harvesting complexes in nature. It has been a subject of numerous experimental and theoretical investigations [24-27]. It shows long lasting quantum coherences with timescales up to 500 fs [24]. Therefore, it is an ideal candidate for study in this fully quantum mechanical model for light-matter interaction. The complete structure of the complex has been studied with X-ray diffraction and other techniques [27]. These studies show that the complex has 3 monomers supported by protein structures. Each monomer contains 14 chlorophylls out of which 6 are chlorophyll b and 8 are chlorophyll a. The structure of a monomer is shown in Figure 38. The average distance between chlorophylls is about 17 to 18 Å [25].

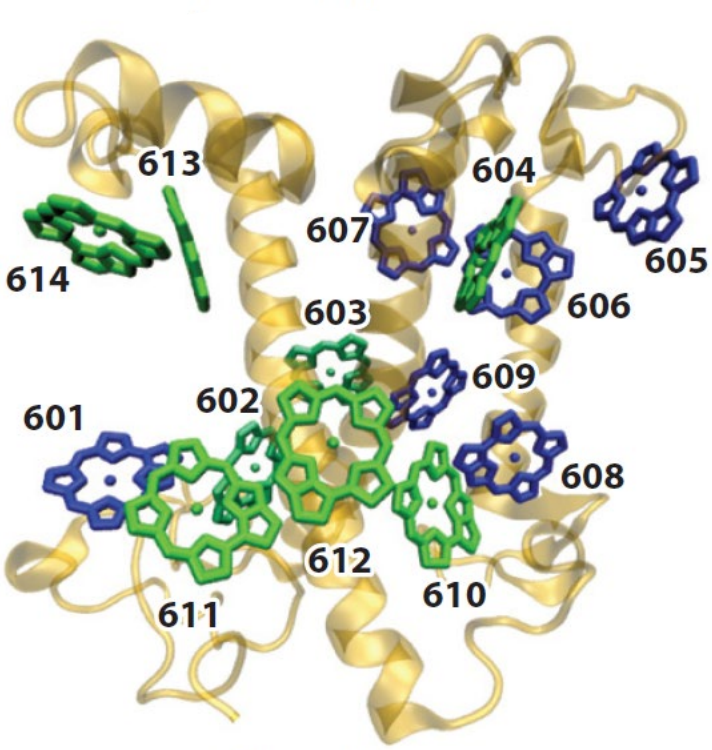

Figure 37: Monomer structure of LHII complex with 8 chlorophyll a (green) and 6 chlorophyll b (blue). The cholorphylls are numbered from 1 to 14 using 6XX notation for XXth chlorophyll. Only the rings containing the magnesium ions are colored as they are the active sites for these chromophores. The rest of the protein structure that supports these chromophores is shown in gold. The image as been adapted from the work of A. Ishizaki and G. R. Fleming [25].

The chlorophylls are complex organic molecules that help in capturing of light for different light harvesting organisms. These chromophores convert the photonic energy into excitonic energy at Mg^{++} ions that are supported in ring-like structure in the chlorophylls. The structures of chlorophyll a and chlorophyll b are shown in Figure 39.

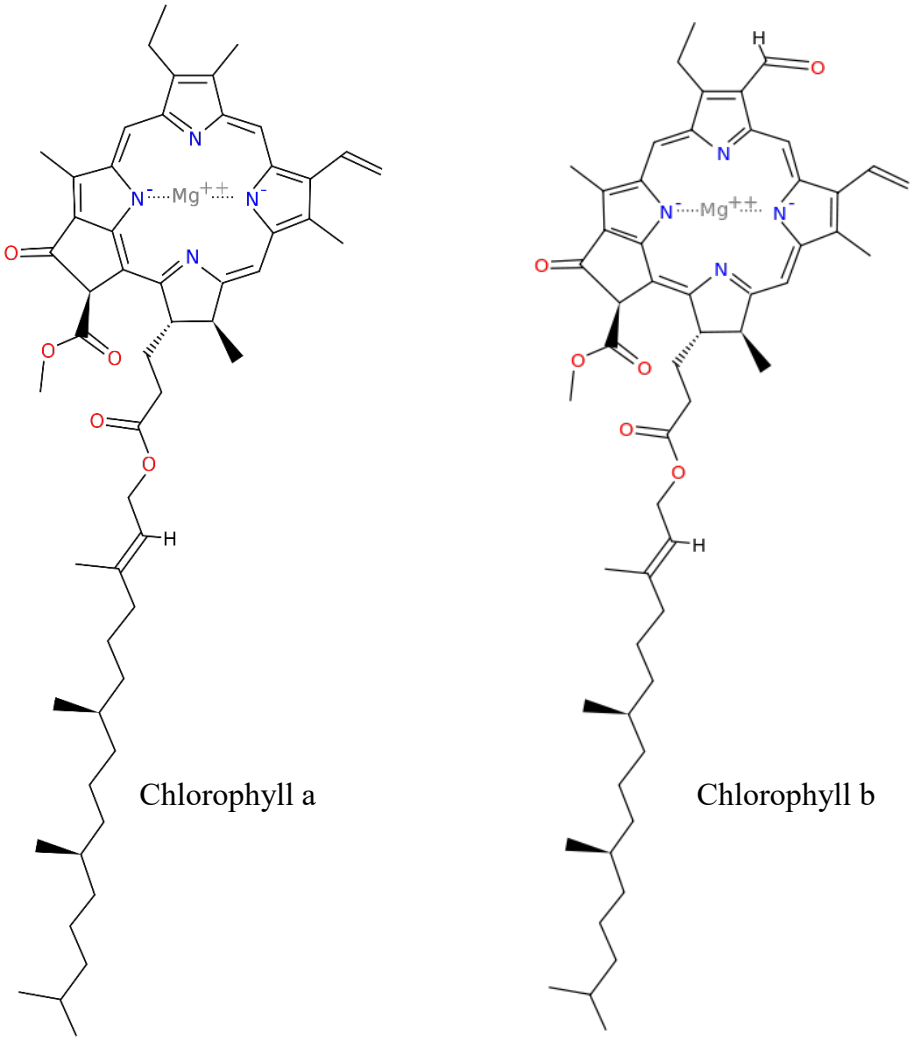

Figure 38: The chemical structures of chlorophyll a and b. The magnesium ions supported in the ring are the sites where photonic energy is absorbed and converted to excitonic energy in these chromophores.

The light-matter interaction of the monomer can be simplified to the interaction of the chlorophyll sites with light and with each other. If the vibronic coupling to the LHII environment and structure is ignored, the Hamiltonian for a monomer coupled to the fundamental mode of the cavity can be written as

$$H_{system} = \hbar\omega_c a^\dagger a + \sum_s \hbar\omega_s b_s^\dagger b_s + \sum_s \hbar g\left(a b_s^\dagger + a^\dagger b_s\right) + \sum_{i,j} \hbar t_{ij}\left(b_i b_j^\dagger + b_i^\dagger b_j\right) + \sum_s \hbar u b_s^\dagger b_s^\dagger b_s b_s \qquad Eq.\,(9.1)$$

Here the summations run from 1 to 14 with sites (chlorophylls) numbered in ascending order with respect to their energy. The site frequencies have been gathered from multiple experimental and theoretical research publications on the LHII complex, they are shown in Figure 40.

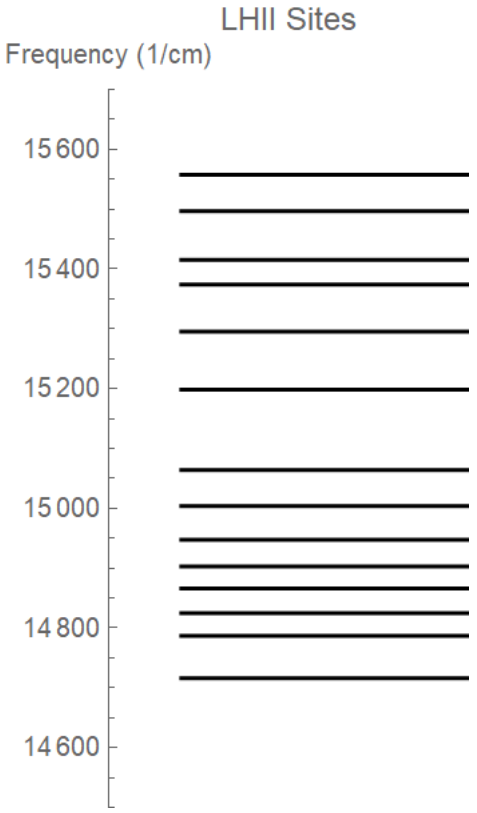

Figure 39: Frequencies for all 14 sites in an LHII monomer. Sites are numbered in ascending order of their frequencies with site 1 at the lowest and site 14 at the highest frequency.

The excitation hoppings are unique for each pair of sites. They are a result of dipole-dipole interaction between different sites and they have been taken from different theoretical and experimental investigations on the LHII complex especially the work of T. Renger et al [26]. The are presented in Table 2 and Figure 41 shows a graphical representation of the hopping network.

Table 2: Hopping matrix for site-site excitation exchange

Site	1	2	3	4	5	6	7	8	9	10	11	12	13	14
1		36	-5	-3	1	-2	-3	3	4	-5	20	2	-8	2
2		0	15	6	0	5	6	-6	-24	-5	1	8	-2	0
3				-1	0	-4	6	4	72	7	-1	1	1	-5
4					4	71	24	-4	-2	0	-3	3	2	-3
5						9	-4	-4	0	1	1	-2	-1	0
6							16	-5	2	0	-2	2	2	-2
7								-4	-5	1	-2	3	3	-3
8									24	43	5	-1	-2	1
9										-2	4	-2	-2	2
0											-26	13	6	-1
11												99	-3	1
12													0	0
13														-36

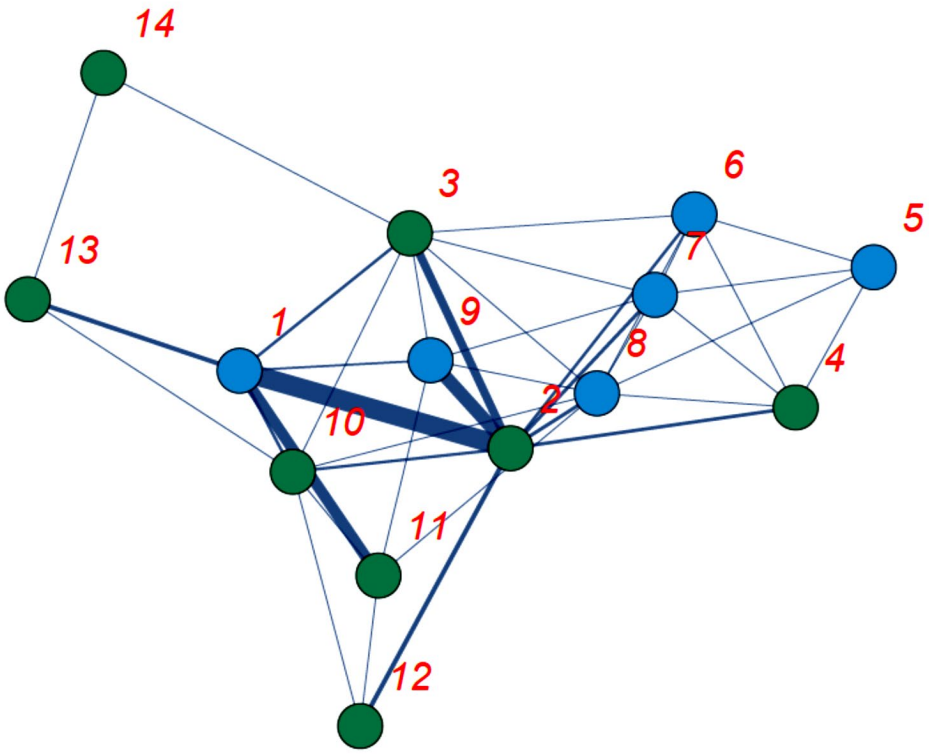

Figure 40: Mapping of chromophores to connected lattice graph. The structure of the graph is not related to the actual spatial position of sites in the LHII complex. The vertices are colored according to chromophore type: green for chlorophyll a and blue for chlorophyll b. The thickness of the edges connecting the vertices give indication of the coupling between sites. The vertices are labeled according to their relative site energies with site 1 having the lowest energy and site 14 having the highest.

For the cavity system described earlier, if the LHII complex is placed inside the cavity, the possible states are shown in Figure 42. These states assume that

$$N_{photons} + N_{excitons} \leq 2$$

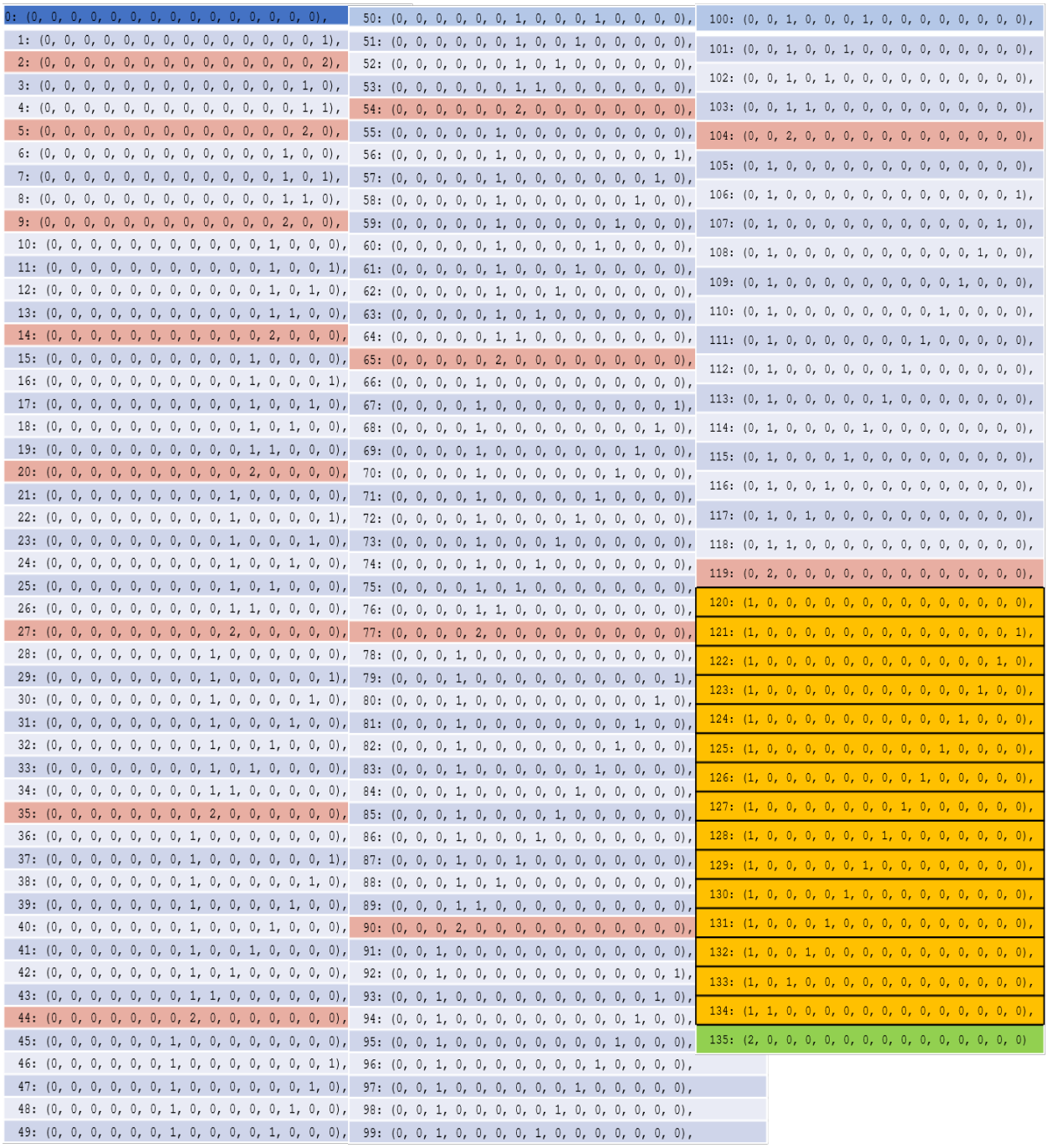

Figure 41: Possible states for the LHII monomer in optical cavity. The states are numbered from 0 through 135. The states are in number basis with $|\psi\rangle = (n_{cavity}, n_{site1}, \dots, n_{site14})$. *The states in red have 2 excitations on a single site, states in yellow have one photon in cavity mode and the last green state has 2 photons in the cavity mode.*

There are 136 states in total with 1 ground state, 15 states with a single excitation on any of the site or photon in cavity, 15 states with double excitations and 105 states with two single excitation on sites and/or cavity mode. Using these states as a basis, the different components of the Hamiltonian are shown in figures . The cavity frequency is $\omega_c = (\omega_{site1} + \omega_{site2})/2$. For this simulation $g = 30\ cm^{-1}$ and $u = 50\ cm^{-1}$. The value of the anharmonicity as been taken from the work of Novoderezkin et al [28-30]. All the frequencies are in wavenumber per centimeter and the energies are in electron volts.

Starting with 2 photon Fock state $|\psi_0\rangle = \left(n_{cavity}, n_{site1}, \dots, n_{site14}\right) = (2, 0, 0, \dots, 0)$, the system evolved under the master equation. The population dynamics inside the cavity is shown in Figure 43. The trends shown that site 9 (ω_{site9} =) gains the most exciton population possibly due to the similarity of its frequency with the cavity frequency (ω_c = 15136.83 cm^{-1}). The first order correlation and spectrum are shown in Figure 44. The spectrum shows two dominant peaks one at site 9 frequency and the other at the new cavity frequency. In the second order correlation presented in Figure 45, there is an interesting peak around 900 fs.

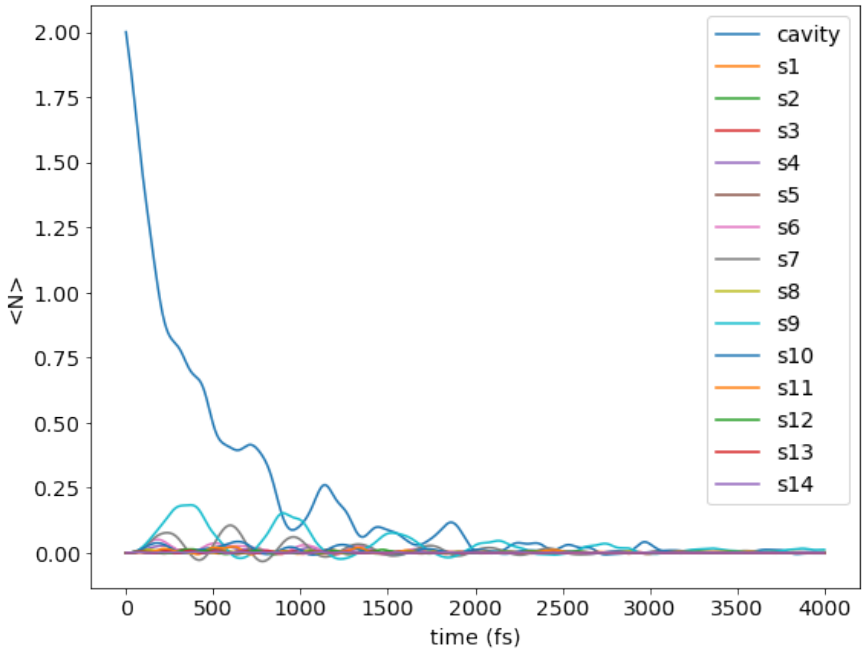

Figure 42: Population dynamics for the LHII monomer inside the cavity with $\omega_c = (\omega_{s1}+\omega_{s2})/2 = 15136.83\ cm^{-1}$.

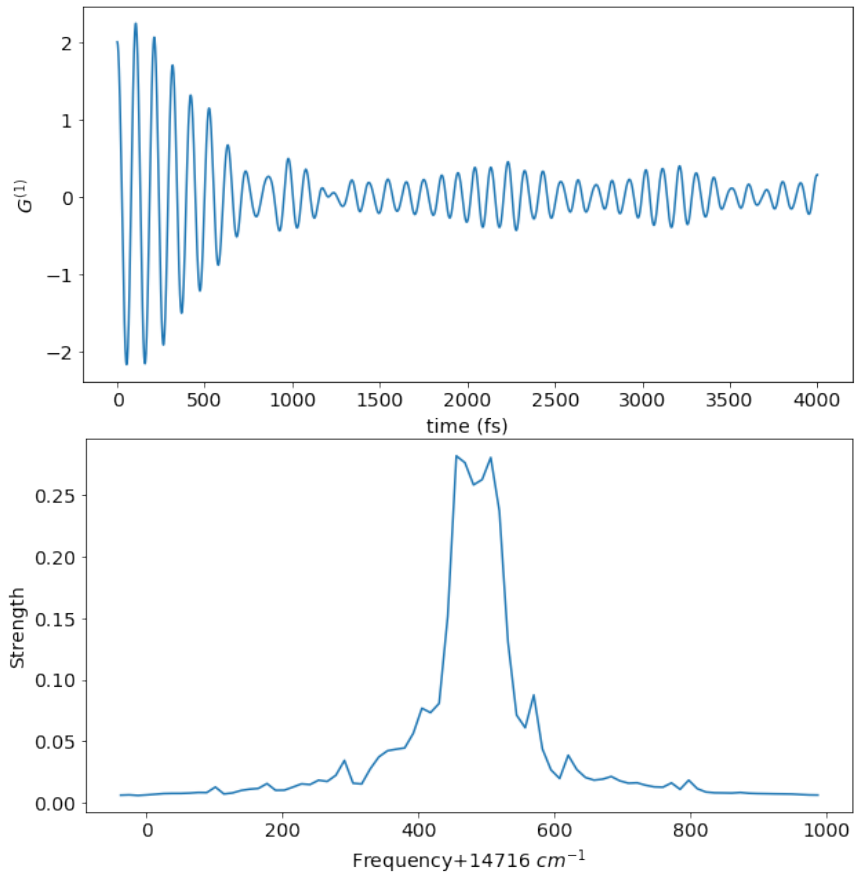

Figure 43: The first order correlation and the associated frequency spectrum for the LHII monomer inside the cavity.

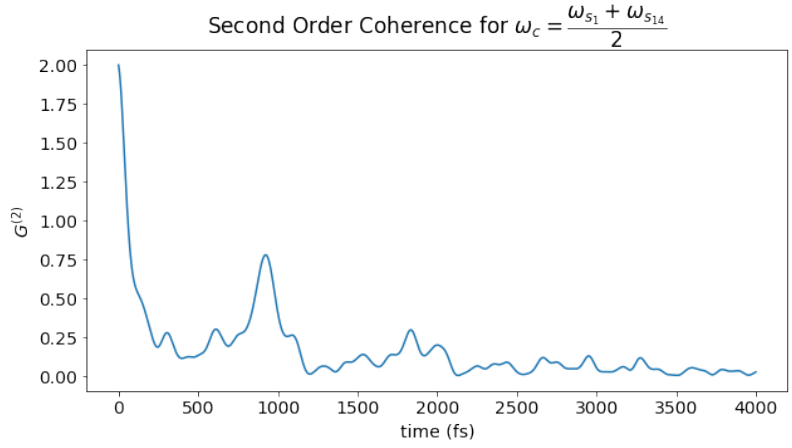

Figure 44: The second order correlation for the LHII monomer in the optical cavity.

Extension to Full LH-II

The discussion so far has focused on a single monomer in the LHII complex. However, the complex contains three monomers. The most straight forward path to formulate the inter-monomer interaction is to work in the eigen-basis for

$$H = \sum_m \hbar\Omega_m \left(B_{m1}^\dagger B_{m1} + B_{m2}^\dagger B_{m2} + B_{m3}^\dagger B_{m3}\right) + \sum_{\mu,\nu} \hbar T_{\mu\nu}\left(B_{m\mu}^\dagger B_{m\nu} + B_{m\nu}^\dagger B_{m\mu}\right)$$
$$+ \hbar g\left(a\left(B_{m1}^\dagger + B_{m2}^\dagger + B_{m3}^\dagger\right) + a^\dagger(B_{m1} + B_{m2} + B_{m3})\right) + \hbar\omega_c a^\dagger a$$

The Heisenberg equations of motion for the a and B are given by

$$i\hbar\frac{\partial a}{\partial t} = \hbar\omega_c a + \hbar g(B_{m1} + B_{m2} + B_{m3}) - i\gamma a$$

and

$$i\hbar\frac{\partial B_\mu}{\partial t} = \hbar\Omega_\mu B_\mu + \sum_\nu \hbar T_{\mu\nu} B_\nu \; + \hbar g a$$

The last term in the expression for a is due to the photon leakage from the cavity with the leakage rate γ. In the expression for B_μ, the last term encodes the interaction between the three monomers of an LHII complex. Since the sites and the monomers act as dipoles, the site-site interaction and monomer-monomer interaction are dipole-dipole interactions. If the distance between sites is described by r and the distance between monomers is represented by R, then from the structure studies of the LHII complex we have

$$r \ll R$$

As the dipole-dipole interactions scale as $\frac{1}{r^3}$; therefore,

$$t \gg T$$

Which implies that the site-site hopping inside a monomer is much bigger factor in determining the dynamics of the system than the inter-monomer interaction. Therefore the inter-monomer coupling can be assumed to be a simple decoherence term that does not affect the dynamics of the system that much.

CHAPTER 10: CONCLUSION AND FUTURE DIRECTION

The systematic study of one and two sites inside the optical cavity has shown that the population dynamics inside the cavity along with correlations and spectrum of the output photons are affected by the intra-material interactions such as hopping (dipole-dipole coupling) and anharmonicity. Furthermore, with a complex sample such as the LHII monomer, the intra-material interactions can be quantitatively analyzed from their signatures on the spectrum and correlations of the output photons in a relatively simple set of experiments.

A number of approximations have been made in this analysis. The thermodynamic coupling of the sites to their surrounding phononic modes (vibrations) has been ignored. Such coupling introduces new collapse operators, which can affect the population dynamics, correlations and spectral features of these systems. For LHII system, these couplings can be introduced in future studies. Furthermore, this analysis can be extended to other chemical system in further work.

Another important restriction has been the removal of the constant pumping of the cavity mode. If the cavity mode is constantly pumped to maintain a certain population of photons, the dynamics can change. These concerns can be easily addressed in future work by the introduction of a photon creation operator based collapse operator. In that case, the system will reach a steady state solution and the most natural basis for such system will be the polariton basis. However, in the current case the cavity and site occupation basis were utilized because the systems have always been in transient state due to the absence of continuous pumping.

Furthermore, the Fock states of light used in these formulations are experimentally difficult to produce than the coherent or thermal states; therefore, the inclusion of these states can be a major direction for the future efforts. The coherent state is the typical state of laser light and it can be included by using its expression in terms of Fock basis, as introduced earlier.

BIBLIOGRAPHY

1. Demtröder, W., *Laser Spectroscopy: Basic Concepts and Instrumentation*. 3 ed. 2002: Springer Science & Business Media. 986.
2. Ameh, E.S., *A review of basic crystallography and x-ray diffraction applications.* The International Journal of Advanced Manufacturing Technology, 2019. **105**: p. 13.
3. Zhang, Z., et al., *Monitoring polariton dynamics in the LHCII photosynthetic antenna in a microcavity by two-photon coincidence counting.* Journal of Chemical Physics, 2018. **148**(7): p. 074302.
4. Schlawin, F., K.E. Dorfman, and S. Mukamel, *Entangled two-photon absorption spectroscopy.* Accounts of Chemical Research, 2018. **51**(9): p. 2207-2214.
5. Li, H., et al., *Photon entanglement entropy as a probe of many-body correlations and fluctuations.* Journal of Chemical Physics, 2019. **150**(18): p. 184106.
6. Kalashnikov, D.A., et al., *Quantum interference in the presence of a resonant medium.* Scientific Reports, 2017. **7**(1): p. 11444.
7. Bittner, E.R., et al., *Probing exciton/exciton interactions with entangled photons: Theory.* Journal of Chemical Physics, 2020. **152**(7): p. 071101.
8. Kalashnikov, D.A., et al., *Quantum interference in the presence of a resonant medium.* Scientific Reports, 2017. **7**(1): p. 11444.
9. Kalashnikov, D.A., et al., *Infrared spectroscopy with visible light.* Nature Photonics, 2016. **10**(2): p. 98-101.
10. Scully, M.O. and M.S. Zubairy, *Quantum Optics*. 1997, Cambridge ; New York: Cambridge University Press. xxi, 630 p.
11. Fox, M., *Quantum Optics : An Introduction*. Oxford master series in physics. 2006, Oxford ; New York: Oxford University Press. xvii, 378 p.
12. Spano, F.C., *Optical microcavities enhance the exciton coherence length and eliminate vibronic coupling in J-aggregates.* The Journal of Chemical Physics, 2015. **142**(18): p. 184707.
13. Herrera, F. and F.C. Spano, *Cavity-controlled chemistry in molecular ensembles.* Physical Review Letters, 2016. **116**(23): p. 238301.
14. Shalabney, A., et al., *Coherent coupling of molecular resonators with a microcavity mode.* Nature Communications, 2015. **6**(1): p. 5981.
15. Kowalewski, M., K. Bennett, and S. Mukamel, *Non-adiabatic dynamics of molecules in optical cavities.* The Journal of Chemical Physics, 2016. **144**(5): p. 054309.
16. Ebbesen, T.W., *Hybrid light–matter states in a molecular and material science perspective.* Accounts of Chemical Research, 2016. **49**(11): p. 2403-2412.
17. Kowalewski, M., K. Bennett, and S. Mukamel, *Cavity femtochemistry: manipulating nonadiabatic dynamics at avoided crossings.* The Journal of Physical Chemistry Letters, 2016. **7**(11): p. 2050-2054.
18. Lindblad, G., *On the generators of quantum dynamical semigroups.* Communications in Mathematical Physics, 1976. **48**(2): p. 119-130.
19. Loudon, R., *The Quantum Theory of Light*. 1979: Oxford University Press.
20. Milonni, P.W., *The Quantum Vacuum: An Introduction to Quantum Electrodynamics*. 1994: Academic Press.
21. Boyd, R., *Nonlinear Optics*. 3rd ed. 2008: Academic Press.

22. Johansson, J.R., P.D. Nation, and F. Nori, *QuTiP 2: A Python framework for the dynamics of open quantum systems.* Computer Physics Communications, 2013. **184**(4): p. 1234-1240.
23. Johansson, J.R., P.D. Nation, and F. Nori, *QuTiP: An open-source Python framework for the dynamics of open quantum systems.* Computer Physics Communications, 2012. **183**(8): p. 1760-1772.
24. Zhang, Z., et al., *Monitoring polariton dynamics in the LHCII photosynthetic antenna in a microcavity by two-photon coincidence counting.* The Journal of Chemical Physics, 2018. **148**(7): p. 074302.
25. Ishizaki, A. and G.R. Fleming, *Quantum coherence in photosynthetic light harvesting.* Annual Review of Condensed Matter Physics, 2012. **3**: p. 28.
26. Müh, F., M.E.-A. Madjet, and T. Renger, *Structure-based identification of energy sinks in plant light-harvesting complex II.* The Journal of Physical Chemistry B, 2010. **114**(42): p. 13517-13535.
27. Zhenfeng Liu, et al., *Crystal structure of spinach major lightharvesting complex at 2.72A° resolution.* Nature, 2004. **428**: p. 4.
28. Novoderezhkin, V., et al., *Exciton modeling of energy-transfer dynamics in the LHCII complex of higher plants: a redfield theory approach.* The Journal of Physical Chemistry B, 2003. **107**(8): p. 1893-1912.
29. Novoderezhkin, V.I., et al., *Energy-transfer dynamics in the LHCII complex of higher plants: modified redfield approach.* The Journal of Physical Chemistry B, 2004. **108**(29): p. 10363-10375.
30. Becker, M., V. Nagarajan, and W.W. Parson, *Properties of the excited singlet states of bacteriochlorophyll a and bacteriopheophytin a in polar solvents.* Journal of the American Chemical Society, 1991. **113**(18): p. 6840-6848.

APPENDIX

```
import matplotlib.pyplot as plt
import matplotlib.animation as animation
import matplotlib.colors as mcolors
import numpy as np
import pandas
from qutip import*

# defining some constants
# h = 4.135667696 eV.fs
# E = hf = hcf/c = hcv where v is the frequency in wavenumber. This eq gives energy in eV from freq in 1/cm.
# c needs to be in cm/fs, c=299792458 m/s = 2.99792458E8 * E-15 * E2 cm/fs = 2.99792458E-5 cm/fs

# units: Energy E = eV,
# freq. v = 1/cm,
# speed of light c = cm/fs,
# h = eV.fs
# time = fs but there is a factor of 2pi since the energies are in hcv and the time-evolution of S.E. has exp(-iEt/hbar)

h_0 = 4.135667696
c = 2.99792458E-5
h = h_0*c
vb_all_ref = [[14750, 14699, 14700], [14840, 14751, 14770], [14860, 14804,
  14810], [14860, 14858, 14880], [14880, 14918, 14910], [14900, 14952, 14990], [14990, 14992, 15030], [15040, 15022,
  15130], [15175, 15210, 15210], [15290, 15306, 15290], [15400, 15363, 15360], [15400, 15416, 15430], [15555, 15456,
  15480], [15650, 15512, 15510]]
vb = []
for x in range(len(vb_all_ref)):
    vb.append(np.mean(vb_all_ref[x])-14716)

t = pandas.read_csv('LHCII_couplings.csv')


class system:
    def __init__(self, total_photons,nphoton,nsite,g,u):
        # total_photons is the max number of photons that can be put in any subsystem
        # nphoton is the number of photons in the starting fock state for the cavity mode.
        # nsite is the number of sites you want to put in the system
        # g is the cavit-site coupling in wavenumbers (1/cm)
        # u is the site anharmonicity (energy cost) in wavenumbers (1/cm)
```

```
        self.total_photons = total_photons
        self.nphoton = nphoton
        self.nsite = nsite
        self.g = g
        self.u = u
        self.state = 'state not defined yet'
        self.H0 = 'H0 not defined here yet'
        self.Hint = 'Hint not defined yet'
        self.a = 'cavity destroy not defined yet'
        self.b = 'site destroy list not defined yet'

        self.set_state(self.nphoton)
        self.set_hamiltonian_and_operators()


    def set_state(self,nphoton):
        self.nphoton = nphoton
        nSubSystems = [self.total_photons+1] # creating a list like [n,n,n,...] so that we can tell
the dimensions to enr_destroy function
        number_state = [self.nphoton]
        for k in range(self.nsite):
            nSubSystems.append(self.total_photons+1)
            number_state.append(0)
        number_state = tuple(number_state)
        print('the state name is ',number_state)
        psi = enr_fock(nSubSystems,self.total_photons,number_state)
        self.state = psi
        return psi

    # The function below, will be developed and used in future.

    def coherent_state(self,nphoton):
        return None
    def thermal_state(self,nphoton):
        return None


    # Now defining Hamiltonian and other operators
    def set_hamiltonian_and_operators(self):

        nSubSystems = [] # creating a list like [n,n,n,...] so that we can tell the dimensions to
enr_destroy function
        for k in range(self.nsite+1):
            nSubSystems.append(self.total_photons+1)
```

```
        all_ops = enr_destroy(nSubSystems,excitations=self.total_photons)
        self.a = all_ops[0]
        self.b = all_ops[1:]

        if self.nsite==1:
            vc = vb[0]
            print('frequencies are ', 'cavity ', vc, 'Site ',vb[0])
            self.H0 = h*vc*self.a.dag()*self.a + h*vb[0]*self.b[0].dag()*self.b[0]   # cavity and
site energies
            self.Hint = h*self.g*(self.a.dag()*self.b[0] + self.b[0].dag()*self.a) # cavity site
Interaction
            # Notice that there is no anharmonicity in this simple system.

        else:
            vc = (vb[0]+vb[self.nsite-1])/2# setting the cav freq to mean of LHII freq range
            print('frequencies are ', 'cavity ', vc, 'First site ',vb[0], 'Last site ', vb[self.nsite-1])

            # First Creating basic hamiltonian
            print('Creating Basic Hamiltonian')
            self.H0 = h*vc*self.a.dag()*self.a   # cavity only
            # Now adding sites
            for m in range(self.nsite):
                name='b'+str(m+1)
                print('adding site energy for ', name)
                b_op = all_ops[m+1]
                self.H0 = self.H0 + h*vb[m]*b_op.dag()*b_op

            # Now Creating Interaction hamiltonian
            print('Now creating Interaction Hamiltonian')
            self.Hint = self.H0-self.H0
            for m in range(self.nsite):
                name='b'+str(m+1)
                print('adding site cavity and anharmonicity for ', name)
                b_op = all_ops[m+1]
                self.Hint = self.Hint +
h*self.g*(self.a.dag()*b_op+self.a*b_op.dag())+h*self.u*(b_op.dag()*b_op.dag()*b_op*b_op
)
            # adding hopping between sites
            for m in range(self.nsite-1):
                name1='b'+str(m+1)
                #print('first',name)
                b_op1 = all_ops[m+1]
                for k in range(m+1,self.nsite):
                    name2 = 'b'+str(k+1)
```

```
                #print('second',name2)
                b_op2 = all_ops[k+1]
                print('adding hopping between sites: ', name1, name2, ' hopping freq t= ',
t.iat[m,k])
                self.Hint = self.Hint+ h*t.iat[m,k]*(b_op1.dag()*b_op2+b_op2.dag()*b_op1)
            print('shape of interaction hamiltonian is', self.Hint.shape)


        return self.H0,self.Hint,self.a,self.b



s0u = system(2,2,2,30,0)
op_list0u = [s0u.a.dag()*s0u.a]
for k in range(len(s0u.b)):
    op0u = s0u.b[k]
    op_list0u.append(op0u.dag()*op0u)

psi_dm0u = s0u.state*s0u.state.dag()
kappa= 0.05**2 # this is the leakage rate, remember the time here is in fs.
c_ops0u = [np.sqrt(kappa)*s0u.a] # just one collapse operator i.e. the leakage rate.

  # time in this simulation is in fs.
tlist = np.linspace(0,4000,4000)
options = Options(store_states = False)
results0u = mesolve(s0u.H0+s0u.Hint, psi_dm0u, tlist, c_ops0u, op_list0u,{},options)

plt.figure(figsize=(10,10))
for m in range(len(results0u.expect)):
    plt.plot(tlist, results0u.expect[m])

plt.legend(['cavity','s1','s2','s3','s4','s5','s6','s7','s8','s9','s10','s11','s12','s13','s14'])
plt.title('Cavity dynamics for a non-interacting cavity')
plt.xlabel('time (fs)')
plt.ylabel('<N>')


n_pop0u = results0u.expect[0]
G1_0u = correlation_2op_1t(s0u.H0+s0u.Hint, psi_dm0u, tlist, c_ops0u, s0u.a.dag(), s0u.a)
g1 = G1 / np.sqrt(n_pop[0] * n_pop)

n_pop0u = results0u.expect[0]
G2_0u= correlation_3op_1t(s0u.H0+s0u.Hint, psi_dm0u, tlist, c_ops0u, s0u.a.dag(),
s0u.a.dag()*s0u.a, s0u.a)
g2 = G2 /(n_pop[0] * n_pop)
```

```
dt = tlist[1]-tlist[0]

FG = scipy.fftpack.fft(G1)
Fg = scipy.fftpack.fft(g1)
freq = fftfreq(len(tlist),dt)
freq = 2*np.pi*fftshift(freq)/h
FG = fftshift(FG)
Fg = fftshift(Fg)


indices = np.intersect1d(np.where(freq>14000), np.where(freq<15500))


plt.figure(figsize=(12,4))
plt.plot(freq[indices], 1.0/len(tlist) * np.abs(FG[indices]))
plt.plot(freq[indices], 1.0/len(tlist) * np.abs(Fg[indices]))
plt.title('Spectrum')
plt.xlabel('Frequency ($cm^{-1}$)')
plt.ylabel('Power')
#plt.grid()
plt.show()
```